© 2018. Published by The Company of Biologists Ltd | Journal of Cell Science (2018) 131, jcs223354. doi:10.1242/jcs.223354

RESEARCH ARTICLE

Mechanically stimulated ATP release from mammalian cells: systematic review and meta-analysis

Nicholas Mikolajewicz[1,2], Ali Mohammed[2], Martin Morris[3] and Svetlana V. Komarova[1,2,*]

ABSTRACT

Body tissues are exposed to a complex mechanical environment, which is perceived by cells and converted to biochemical signals such as ATP release. We performed a meta-analysis of 278 systematically identified studies that investigated mechanically stimulated ATP release (MSAR) to quantify the amounts, kinetics and mechanisms of ATP release under normal and pathological conditions. Mechanically stimulated mammalian cells were shown to release 38.6 [95% confidence interval (CI): 18.2–81.8] amol ATP/cell on average with a characteristic time constant of 32 s (95% CI: 16–66). Analysis of ATP release mechanisms revealed the existence of conserved and tissue-specific release routes. We assessed ATP release in pathophysiological states, and found that ATP release was elevated in inflammation and injury, and attenuated in hereditary (such as cystic fibrosis) and metabolic (such as type II diabetes) conditions. Our study links cell-specific ATP release mechanisms to pathophysiological changes in ATP release and allows ATP release-targeting interventions to be mapped to site-specific effects. This work demonstrates that quantitative synthesis of basic research can generate non-trivial hypotheses and inform evidence-driven translational studies.

KEY WORDS: ATP release, Mechanical stimulation, Meta-analysis, Systematic review

INTRODUCTION

The discovery that mechanical stimuli elicit adenosine triphosphate (ATP) release from mammalian cells was made over 25 years ago (Milner et al., 1990), and represented a paradigm shift in how we understand the interaction between the body and the mechanical environment. The body is constantly exposed to a complex combination of shear forces, strains, osmotic stresses and pressures. These forces are perceived at the cellular level and converted to biochemical signals, one of which involves the release of ATP, a high-energy content purine molecule that represents the primary source of cellular energy (Bergman, 1999). It is now clear that extracellular ATP is as an autocrine and paracrine signaling molecule that exerts its effects through purinergic receptors (Burnstock, 2014).

In this study, we systematically reviewed the literature pertaining to mechanically stimulated ATP release (MSAR) from mammalian cells and conducted a meta-analysis on relevant studies. The primary objective was to provide quantitative estimates of the amount of ATP released and kinetics of this release in response to mechanical stimulation. The secondary objective was to extend our analysis to address problems that are otherwise difficult to investigate at the single-study level, including comparing the effects of different mechanical stimuli, as well as consolidating the available intervention- and pathology-related data. In addition to our research objectives, we sought to demonstrate the feasibility and value of conducting meta-analyses at the basic research level to complement existing lines of evidence used to inform translational research.

RESULTS

Overview of relevant studies

We systematically identified 278 studies that directly measured ATP release from mechanically stimulated mammalian cells, 228 of which were included in quantitative synthesis (50 studies were excluded due to inadequate reporting) (Fig. 1A). In these studies, 9 unique models of mechanical stimulation, including osmotic pressure, fluid shear stress (FSS), strain and compression, were used to stimulate ATP release from mammalian cells (Fig. 1B). Cells derived from 12 different organ systems were studied, most commonly originating from the urinary and musculoskeletal systems (Fig. 1C). Most studies measured ATP using the luciferin-luciferase bioluminescence assay (255/278), while others used high-performance liquid chromatography (11/278), hexokinase-based enzymatic assays (5/278), surface-bound luciferase probes (3/278), microelectrodes (3/278) and cell-based biosensors (1/278). We tracked the discovery of non-lytic ATP release to Milner et al., who described the phenomenon in FSS-stimulated endothelial cells in 1990 (Milner et al., 1990) (Fig. 1D). The physiological relevance of MSAR was soon after realized and widespread interest surged around the 2000s. It is now clear that MSAR is physiologically involved in virtually every organ system and plays a role in facilitating responses to mechanical perturbations that demand immediate physiological feedback (Fig. 1E). To date, the general physiological relevance has been established, and current work in the field is focused on understanding the mechanistic and potential therapeutic relevance of MSAR.

MSAR is a conserved phenomenon in mammalian cells

We quantified ATP release as the amount of ATP liberated into the extracellular space after mechanical stimulation (Fig. 2A). Using a random effects model, we estimated that mechanically stimulated mammalian cells released 38.6 [95% confidence interval (CI) 18.2–81.8] amol ATP/cell over a basal extracellular amount of 8.1 (95% CI: 3.9–16.6) amol ATP/cell. The total intracellular ATP content was estimated to be 5.0 (95% CI: 2.6–9.5) fmol ATP/cell in nucleated cells and 0.14 (95% CI: 0.12–0.18) fmol ATP/cell in red blood cells (RBCs) (Fig. 2B; Table S1). ATP release estimates were

[1]Faculty of Dentistry, McGill University, Montreal, Quebec, Canada, H3A 1G1. [2]Shriners Hospital for Children - Canada, Montreal, Quebec, Canada, H4A 0A9. [3]Schulich Library of Physical Sciences, Life Sciences and Engineering, McGill University, Montreal, Canada, H3A 0C1.

*Author for correspondence (svetlana.komarova@mcgill.ca)

N.M., 0000-0002-7525-0384; S.V.K., 0000-0003-3570-3147

Received 31 July 2018; Accepted 10 October 2018

Journal of Cell Science (2018) 131, jcs223354. doi:10.1242/jcs.223354

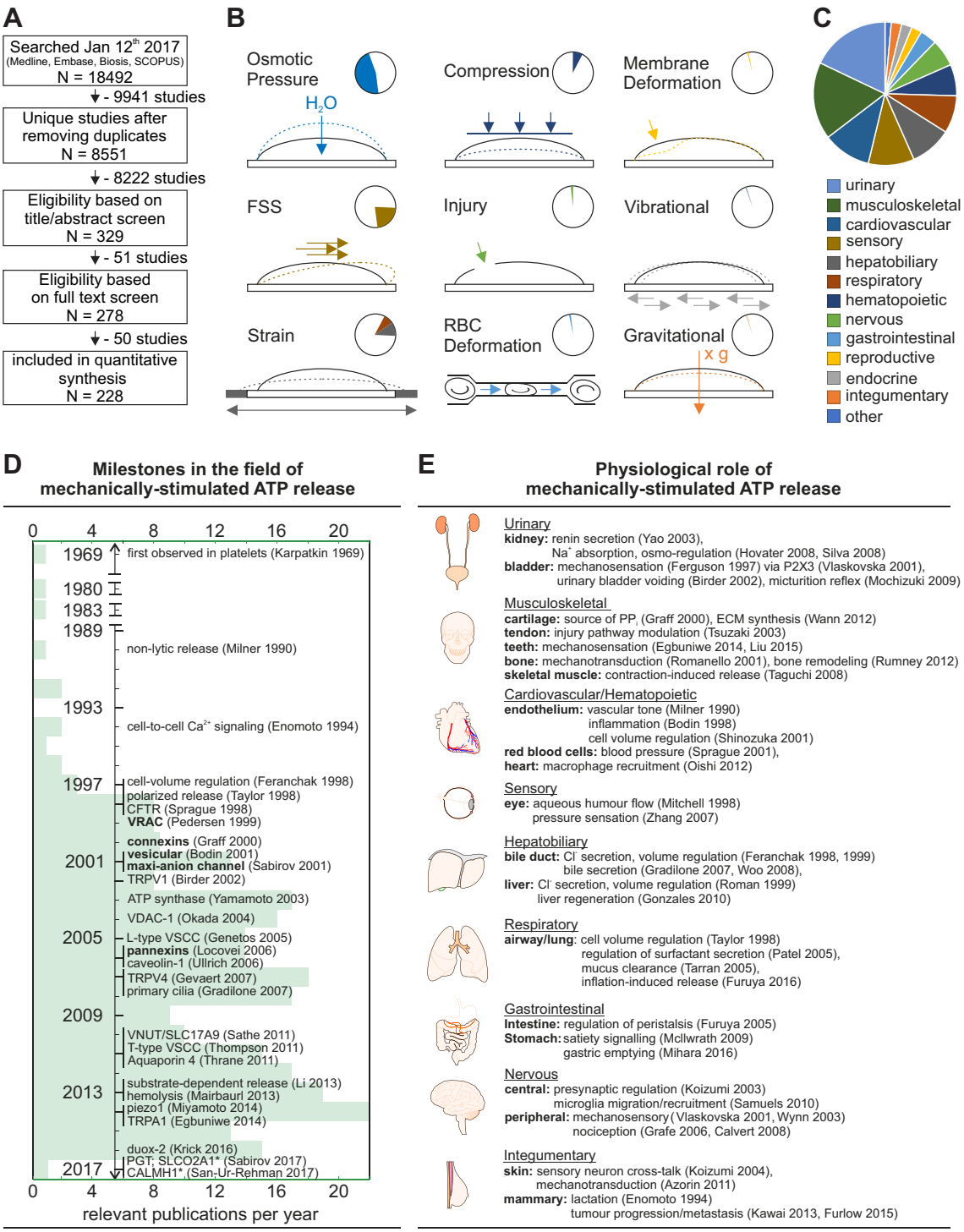

Fig. 1. Overview of studies in the field of MSAR. (A) Simplified PRISMA diagram of the information flow throughout systematic screening process. *N*, number of studies. (B) Schematics of mechanical stimuli studied. Pie charts show the proportion of studies focused on specified mechanical stimulus. Strain includes tissue distension and substrate stretch; vibrational includes ultrasonication and substrate vibration. (C) Pie chart of relative frequency of organ systems studied. (D) Milestones in the field of MSAR. The timeline shows key publications or notable discoveries; main routes of ATP release identified are indicated in bold text; the bar graph (green) shows the number of relevant publications per year; asterisks indicate key contributions published after systematic search. (E) Overview of the physiological role of MSAR in different tissues. CALHM1, calcium homeostasis modulator 1; CFTR, cystic fibrosis transmembrane conductance regulator; ECM, extracellular matrix; FSS, fluid shear stress; g, gravitational force; PGT, prostaglandin transporter; PP_i, pyrophosphate; RBC, red blood cell; VDAC, voltage-dependent anion channel; VRAC, volume-regulated anion channel; VSCC, voltage-sensitive calcium channel; VNUT, vesicular nucleotide transport.

considerably inconsistent between studies, ranging over 10 orders of magnitude (Fig. S1, Table S1). We found that 80% of the heterogeneity was explained by a correlation between basal ATP (A_{base}) and ATP release (A_{mech}) estimates that arose only between studies but was absent within studies (Fig. 2C). Furthermore, we found that heterogeneity in basal ATP was not explained by differences in methodologies (Fig. 2D), suggesting that the primary source of heterogeneity was inconsistent ATP calibrations between

Journal of Cell Science (2018) 131, jcs223354. doi:10.1242/jcs.223354

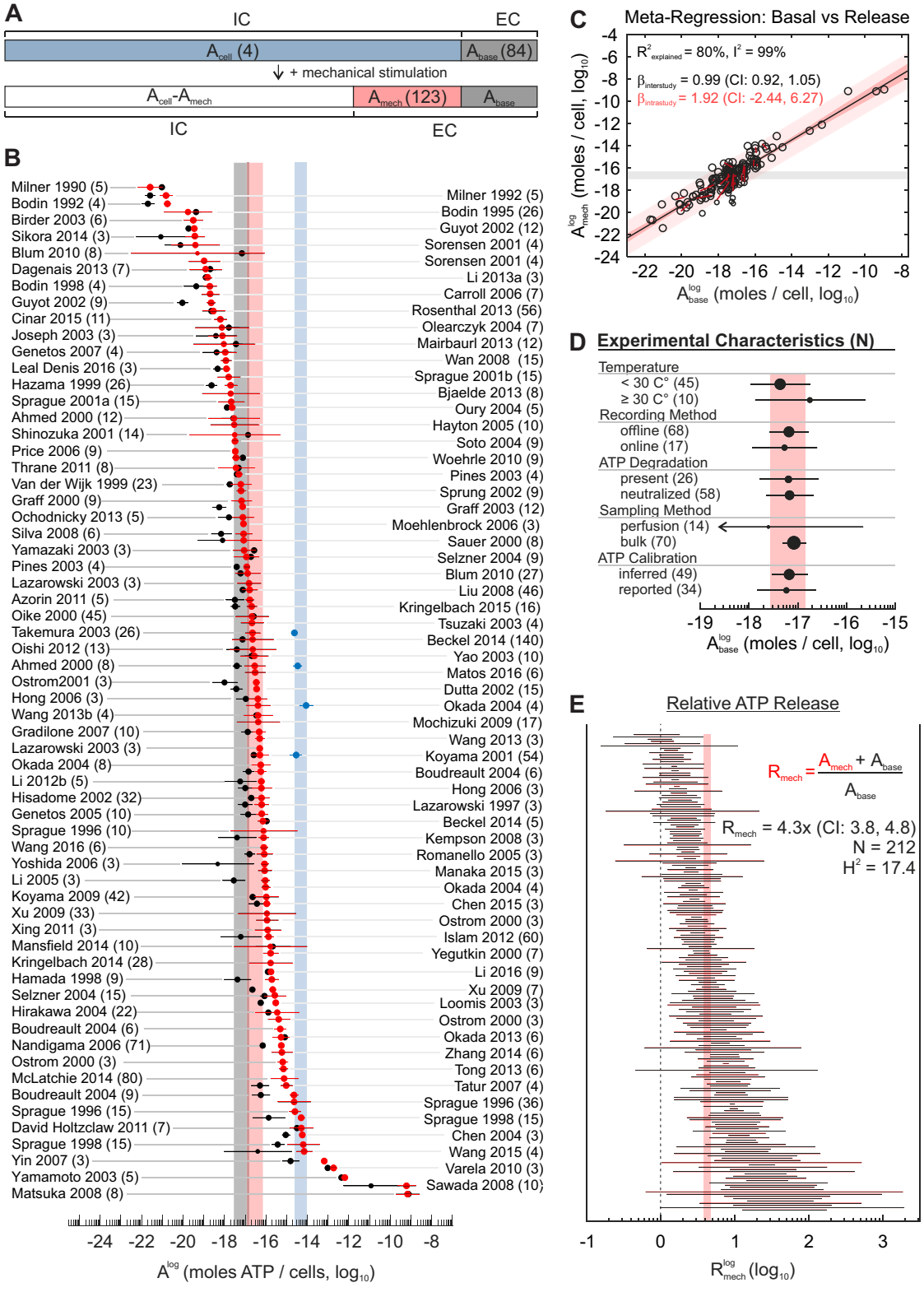

Fig. 2. Quantitative analysis of MSAR from mammalian cells. (A) Schematic representation of intracellular (IC) ATP content (A_{cell}, blue), basal extracellular (EC) ATP (A_{base}, gray) and ATP released by mechanical stimulation (A_{mech}, red). The number of datasets is shown in parentheses. (B) Forest plot of log-transformed study-level outcomes ±95% confidence intervals (CI). The shaded bands indicate 95% CI for overall A^{log}_{cell}(blue), A^{log}_{base} (gray) and A^{log}_{mech} (red). Study-level sample sizes are in parentheses. (C) Meta-regression analysis of the relationship between A^{log}_{base} and A^{log}_{mech}. Black lines indicate meta-regression; dark/light-red bands indicate 95% CI and prediction intervals, respectively; the gray band indicates A^{log}_{mech} 95% CI; red lines indicate within-study regression. $R^2_{explained}$, heterogeneity explained by regression; I^2, variance due to heterogeneity; $\beta_{interstudy}$, slope ±95% of the between-study relationship; $\beta_{intrastudy}$, average slope ±95% of the within-study relationship. (D) Effects of experimental factors on A^{log}_{base}. Black markers/lines indicate subgroup estimates ±95% CI; the red band indicates overall A^{log}_{base} 95% CI. (E) Forest plot of study-level 95% CI for relative ATP release R^{log}_{mech}. The shaded band indicates overall 95% CI for R^{log}_{mech}; the dashed black line is the no ATP released reference. H^2, heterogeneity statistic; *N*, number of included datasets. Detailed overall statistics are provided in Tables S1 and S2.

Journal of Cell Science

studies. Estimates of relative ATP release were more consistent between studies, and were unaffected by the overall quality of the study, although some publication bias was evident (Fig. S1). We found that every cell type investigated responded to mechanical stimulation by releasing ATP, resulting in a 4.3-fold (95% CI: 3.8–4.8) increase in extracellular ATP above baseline (Fig. 2E). Remarkably, the amount of ATP released was generally robust to variations in experimental methodology and biological characteristics (Fig. S2, Table S2). In particular, different cell types, cells from different species, embryonic origin and most organ systems released similar amounts of ATP upon mechanical stimulation. Among the factors that did influence ATP release, we found that neutralization of ATP degradation or application of cyclic mechanical stimuli were associated with relatively lower ATP release (Fig. S2A), and polarized epithelia released significantly higher amounts of ATP from the apical surface compared with the basolateral membrane (Fig. S2B). We conclude that MSAR is a conserved phenomenon in mammalian cells, and provide robust quantitative estimates for the absolute and relative amounts of ATP released upon mechanical stimulation.

The amount of ATP release is proportional to the magnitude of mechanical stimulation

We next investigated the relationship between the type of mechanical stimulation and ATP release. We found that similar amounts of ATP were released in response to all studied mechanical stimuli (Fig. 3A; Table S3). Only locally applied membrane deformations resulted in lower ATP release compared with other forms of stimulation. We used a combination of meta-regression and within-study regression to investigate the relationship between the magnitude of mechanical stimulation and the amount of ATP released (Fig. 3B–G; Table S3). Within studies, ATP release was consistently proportional to the magnitude of mechanical stimulation, whereas between studies this relationship was less pronounced. Nevertheless, the directions of association were consistently positive for all types of mechanical stimulation (Fig. 3H). Thus, despite evident aggregation bias, we conclude that the amount of ATP released is governed by the magnitude of mechanical stimulation.

ATP release kinetics are stimulus dependent

To quantify the kinetics of ATP release, we fitted study-level time-series data to a sigmoidal model using a Monte Carlo fitting procedure and estimated the time to half-maximal (half-max) ATP release t_{half} (Fig. 4A). Meta-analysis demonstrated that the characteristic half-max ATP release time was 101 s (95% CI: 83–117 s) (Fig. 4B). ATP release kinetic estimates were moderately heterogeneous with no discernable publication bias, and they were not influenced by study quality (Fig. S3). However, we found that real-time online recordings of ATP release yielded significantly faster release kinetics of 32 s (95% CI: 16–66 s) compared with offline measurement methods, which yielded slower kinetics of 136 s (95% CI: 117–159 s) (Fig. 4C,D; Table S4). We stratified the data by recording method prior to further analysis. ATP release kinetics were robust to differences in all other experimental factors but not to biological factors (Fig. S4, Table S4). ATP release was relatively slower in certain species (guinea pigs, porcine, rabbits) and cells from different embryonic origins (ectoderm) and organ systems (sensory). Importantly, the kinetics of ATP release depended on the type of mechanical stimulus applied. FSS evoked significantly faster ATP release compared with osmotic pressures (Fig. 4E,F; Table S4). Thus, systematic large-scale data synthesis allowed us to identify a previously unknown relationship between ATP release kinetics and the type of mechanical stimulation, suggesting that it needs to be further explored experimentally.

Mechanisms of MSAR

We next synthesized the data pertaining to the mechanisms of MSAR. Pharmacological and genetic interventions were grouped by common molecular targets (Table S5) and their relative inhibitory effects were quantified for each cell type (Fig. 5; Table S6). The five main direct routes of MSAR that have been identified in mammalian cells are vesicles (Bodin and Burnstock, 2001; Sathe et al., 2011), pannexins (Locovei et al., 2006), connexins (Graff et al., 2000), volume-regulated anion channels (VRACs) (Pedersen et al., 1999; Qiu et al., 2014; Voss et al., 2014) and maxi-anion channels (MACs) (Sabirov et al., 2001; Sabirov et al., 2017). Vesicles were involved in 70% (14/20) of studied cell types from all organ systems except for the integumentary (i.e. keratinocytes, mammary epithelial cells) (Fig. 5A). Pannexins were the second most common route of ATP release, involved in 58% (15/26) of all studied cell types. Pannexin-mediated ATP release occurred in hematopoietic cells, astrocytes and most epithelial cells (including digestive, airway and ocular). Connexins, VRACs and MACs were implicated in ATP release in 35% (7/20), 36% (4/11) and 23% (3/13) of all cells studied, respectively. Connexin-mediated ATP release was highly prevalent in ocular cell types and in the kidney, but was absent in airway epithelia and smooth muscle. VRACs exhibited no discernable tissue-specific pattern of involvement, while MACs were almost exclusively implicated in ATP release from integumentary cells. This data-driven summary of MSAR mechanisms allowed us to establish tissue-level generalizations and suggest the existence of common (vesicular) and tissue-specific (pannexin, connexins, MAC) routes of ATP release.

We conducted a co-occurrence analysis to screen for possibly co-dependent pathways of ATP release (Fig. 5B). The main routes of ATP release (i.e. vesicular, pannexin, connexin, VRAC and MAC) co-occurred pairwise in 27–67% of studied cells, except for vesicle- and MAC-mediated ATP release routes, which were mutually exclusive (co-occurred in 0 of the 4 cell types studied; 0/4). We investigated whether the main routes of ATP release contributed to the total amount of ATP released in an additive manner by accounting for the relative contributions of each route (Table 1). In certain cell types, the total amount of ATP released was accounted for by the additive contribution of the main routes of ATP release. However, in cardiomyocytes, ligament cells, pancreatic and renal epithelia, and urothelial cells, the additive contributions exceeded the amount of ATP released. Although there is a possibility that pharmacological non-specificity contributed to this effect, genetic methods were in agreement. For instance, small interfering RNA (siRNA)-mediated knockdown of Cx43 (also known as GJA1) and Panx1 in ligament cells inhibited ATP release by 73.1% (95% CI: 68.7–77.4) (Luckprom et al., 2011) and 73.6% (95% CI: 69.2–78.0) (Kanjanamekanant et al., 2014), respectively. These findings suggest the existence of a cell type-specific synergistic interaction between ATP release routes previously thought to be functionally independent.

We investigated the association between the main ATP release routes and other implicated regulatory and auxiliary pathways. Vesicular ATP release consistently coincided with the involvement of intracellular calcium ($[Ca^{2+}]_i$, 8/8 cell types studied), Rho kinases (3/3) and microtubules (4/4). Rho kinases (3/3) and microtubules (3/3) were also involved in pannexin-mediated ATP release. No pathway consistently co-occurred with connexin-mediated

Journal of Cell Science (2018) 131, jcs223354. doi:10.1242/jcs.223354

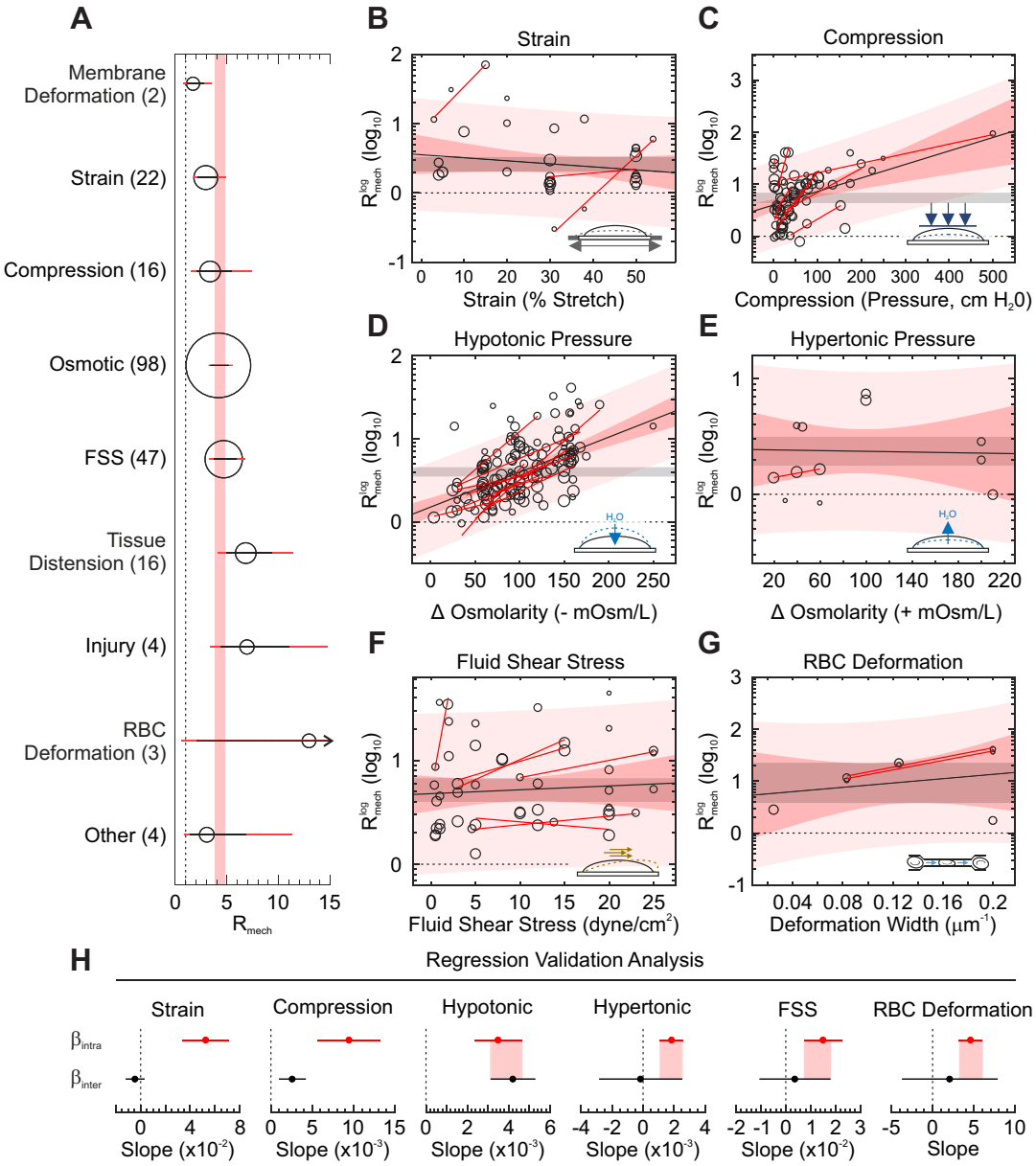

Fig. 3. Relationship between mechanical stimuli and ATP release. (A) Relative amount of ATP (R_{mech}) released in response to different mechanical stimuli. The number of datasets is shown in parentheses. Black circles indicate subgroup estimates; horizontal black lines indicate ±95% CI; horizontal red lines indicate ±Bonferroni-adjusted 95% CI; the red band indicates 95% CI for overall R_{mech}; the dashed black line is the no ATP released reference. (B–G) Meta-regression analysis of the relationship between the magnitude of mechanical stimulation and R^{log}_{mech} following stimulation by strain (B), compression (C), hypotonic pressure (D), hypertonic pressure (E), FSS (F) or deformation of RBCs (G). Black lines indicate meta-regression; dark/light-red bands indicate 95% confidence and prediction intervals; gray bands indicate 95% CI of R^{log}_{mech} for the indicated stimulus; red lines indicate intrastudy regression. Insets are schematics of mechanical stimuli. (H) Comparison of intrastudy (β_{intra}, red) and interstudy (β_{inter}, black) regression slopes ±95% CI. Red bands indicate 95% CI overlap; dashed lines are the no relationship reference. Detailed statistics are provided in Table S3.

ATP release. VRAC-mediated ATP release coincided with the involvement of P2X7 receptors (5/5), but never with ATP synthase (0/3), and MAC-mediated ATP release co-occurred with ATP synthase-related ATP release (3/3), but never with $[Ca^{2+}]_i$-dependent ATP release (0/3). Thus, we have identified conserved cell-independent signaling patterns that warrant further experimental investigation.

We next explored whether the mechanisms of ATP release depend on the type of mechanical stimulation (Fig. 5C). We examined the contribution of the main routes of ATP release in response to mechanical stimuli with sufficiently large datasets (FSS, osmotic pressure and strain). All 5 routes of ATP release were implicated in osmotic pressure- and strain-induced ATP release with the similar patterns of contribution. In contrast, VRAC and possibly pannexins were not involved in FSS-induced ATP release. Thus, consistent with our findings that FSS- and osmotic pressure-induced ATP release exhibit distinct release kinetics, these data suggest that distinct mechanisms may contribute to stretch- and shear-related responses.

MSAR in pathologies

Aberrant ATP release has been implicated in multiple pathophysiological conditions (Fig. 6A). Inflammation- and

Journal of Cell Science (2018) 131, jcs223354. doi:10.1242/jcs.223354

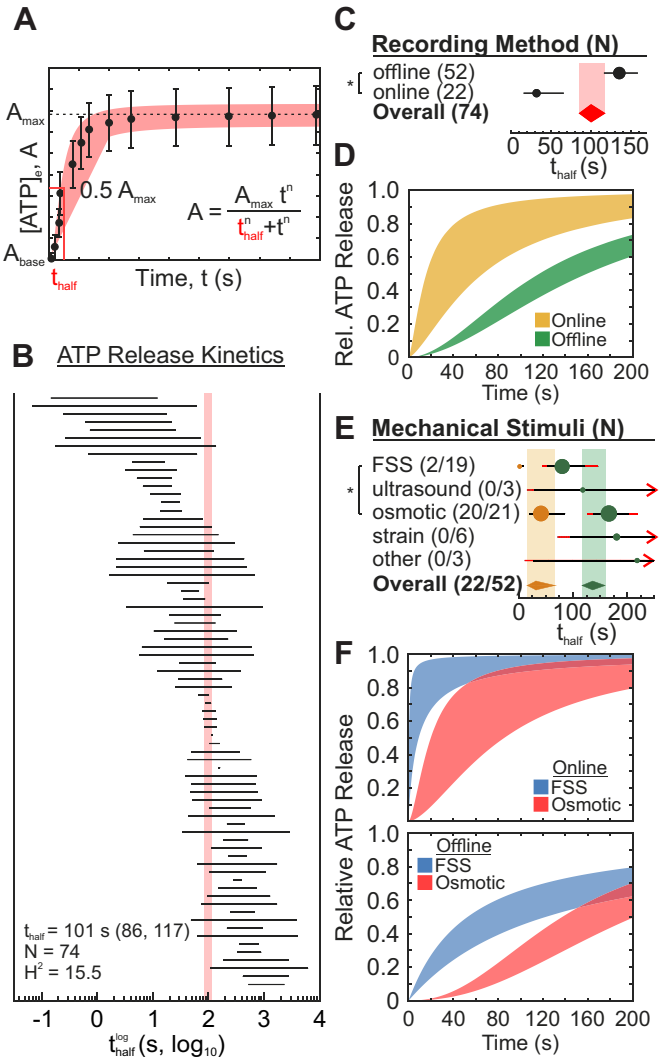

Fig. 4. Kinetics of ATP release. (A) Study-level ATP release kinetics (black circles) were fit to sigmoidal function using the Monte Carlo method and characteristic time to half-max release (t_{half}, red) with standard error was estimated. The dashed black line indicates the maximal ATP released (A_{max}); the red band indicates sigmoidal function 95% CI. (B) Forest plot of log-transformed study-level 95% CIs for t_{half} (t_{half}^{log}). The shaded band indicates the 95% CI for overall t_{half}^{log}. *N*, number of datasets; H^2, heterogeneity statistic. (C,D) Subgroup estimates of t_{half}±95% CI (C) and 95% CI temporal profiles of ATP release (D) recorded using online or offline methods. The red band indicates the 95% CI for overall t_{half}. (E,F) t_{half} stratified by recording method for different mechanical stimuli. (E) Subgroup t_{half} estimates. Green, offline recording; yellow, online recording; horizontal black lines, ±95% CI; horizontal red lines, ±Bonferroni-adjusted 95% CI; bands/diamonds, overall t_{half} ±95% CI. (F) Comparison of FSS- (blue) and osmotic pressure- (red) stimulated ATP release 95% CI temporal profiles when recorded online (top) or offline (bottom). Detailed statistics are in Table S4.

injury-related conditions were associated with elevated levels of MSAR, compared with unaffected controls (Fig. 6B; Table S7). On the other hand, attenuated ATP release was observed in hereditary conditions, such as cystic fibrosis and xerocytosis, and in type II diabetes and primary pulmonary hypertension (Fig. 6C; Table S7). In some pathologies, the magnitude or direction of changes in MSAR were specific to the cell or stimulus. In cystic fibrosis, RBCs and pancreatic epithelia released less ATP upon stimulation, while airway epithelia and astrocytes were unaffected. Acute hypoxia potentiated ATP release from endothelial cells, while chronically hypoxic cells released less ATP (Fig. 6D; Table S7). In polycystic kidney disease (PKD), renal epithelia released less ATP upon FSS stimulation in both autosomal dominant and recessive cases, whereas osmotic swelling-induced ATP release was unaffected in autosomal recessive and potentiated in autosomal dominant PKD (Fig. 6D; Table S7), again suggesting distinct cell processing of shear- and stretch-related stimuli. Thus, we demonstrate the presence of specific patterns of MSAR alteration with respect to the type of pathology, affected cells and applied stimulus, and suggest that inhibitory and stimulatory interventions targeting MSAR can be of therapeutic interest, but need to be applied with caution. Our study maps the potential anatomical sites and situations in which targeting MSAR could have (patho-)physiological consequences.

DISCUSSION

Overview

We have conducted a systematic large-scale data synthesis to quantitatively characterize the amounts, kinetics and mechanisms of MSAR under normal and pathological conditions. From 228 systematically selected studies, we extracted 123 estimates of absolute and 212 estimates of relative amount of ATP released, 74 kinetic time-series, 592 pharmacological and 89 genetic intervention outcomes, and 51 pathophysiological comparisons. Using a meta-analytic approach, we have established that mechanically stimulated mammalian cells release 38.6 (95% CI: 18.2–81.8) amol ATP/cell, with a characteristic time constant of 32 s (95% CI: 16–66) measured using real-time recording methods. We have found that MSAR is a universally conserved phenomenon in mammalian cells, and that cells from different species, embryonic origin and most organ systems release similar amounts of ATP when mechanically stimulated. Our data-driven summary of MSAR mechanisms allowed us to infer tissue-level generalizations that suggest the existence of common and tissue-specific routes of ATP release, and to identify conserved cell type-independent signaling patterns. We have found that inflammation and injury were associated with increased MSAR, whereas hereditary and metabolic conditions resulted in attenuated ATP release. Importantly, several lines of evidence including (1) differences in release kinetics, (2) implicated mechanisms and (3) pathophysiological effects in PKD, suggest that cells can discriminate between stretch- and shear-related forces. Thus, consolidating and quantifying over 25 years of basic research data generated in 64 unique cell types derived from 12 organ systems and stimulated by 9 distinct force applications allowed us to generate novel testable hypotheses, and provide evidence-driven recommendations for translational studies.

Study limitations

The studies included in this meta-analysis were highly heterogeneous; however, this was expected due to the higher methodological variability in exploratory basic science studies (Bradbury and Plückthun, 2015; Fontoura-Andrade et al., 2017; Soehnlein and Silvestre-Roig, 2017). Importantly, accounting for interstudy differences in ATP calibration and recording methods allowed us to dramatically reduce heterogeneity. We found minimal evidence of publication bias. We also demonstrated that the quality of the studies did not significantly affect study-level outcomes, despite quality scores varying substantially across studies. It is known that subgroup analyses come at the expense of lower statistical power; however, the large number of available datasets permitted statistically powered analysis for numerous secondary outcomes (Jackson and Turner, 2017). Analysis of MSAR

Journal of Cell Science (2018) 131, jcs223354. doi:10.1242/jcs.223354

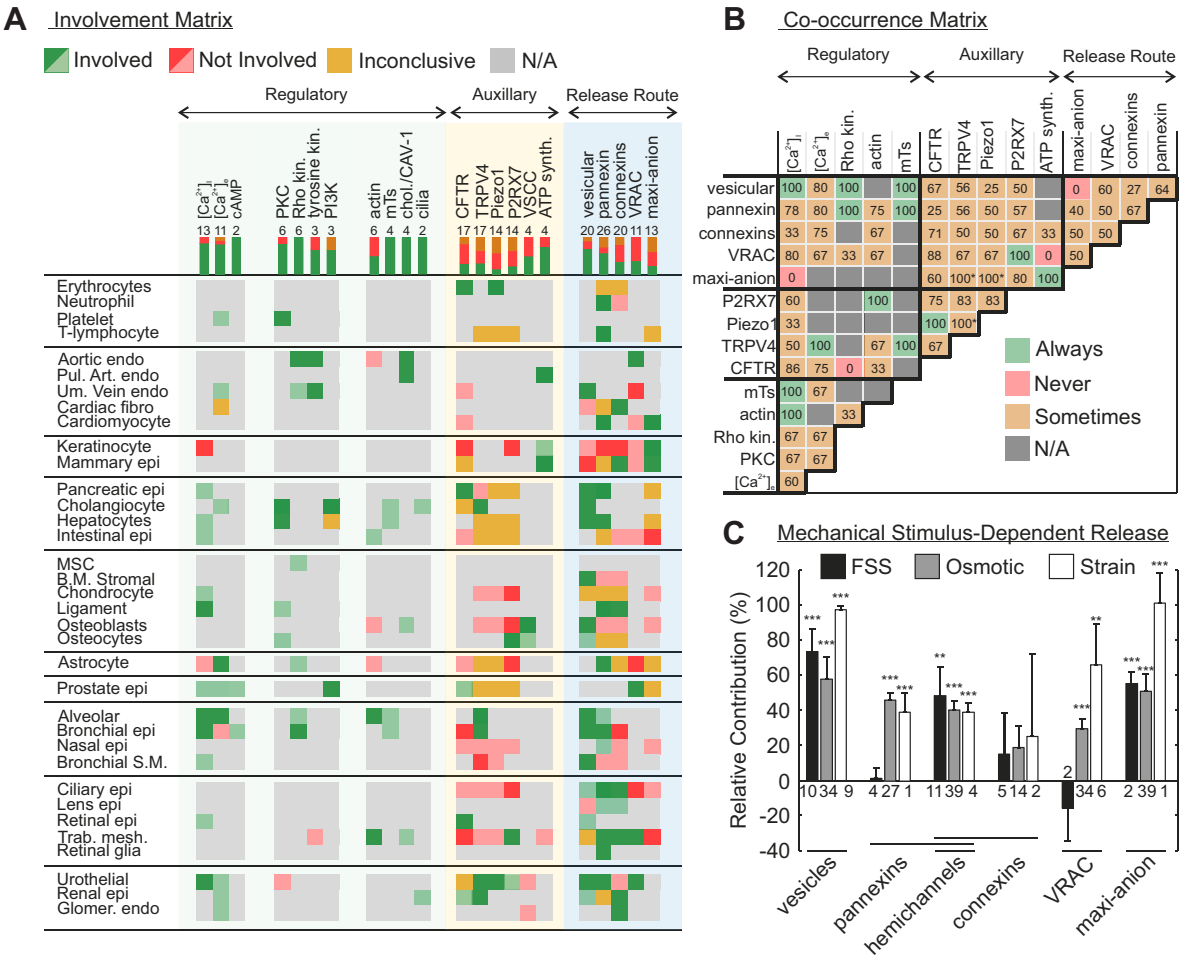

Fig. 5. Mechanisms of MSAR. (A) Involvement of the most commonly studied MSAR mechanisms (columns) for each cell type (rows). Stacked bars indicate the relative frequencies of involvement for each mechanism. The number of unique cell types studied per mechanism is indicated. Dark green/red indicates findings replicated by a separate study/method; light green/red indicates findings that are not replicated. (B) Percentage of cell types in which implicated mechanisms co-occurred. Results shown are for mechanism pairs studied in >2 cell types. Asterisks indicate pairwise co-occurrences confounded by common pharmacological interventions. (C) Relative contributions of main ATP release routes to ATP release in cells stimulated by FSS, osmotic pressure or strain, approximated by inhibitory effect (%)±s.e. of interventions. ***P*<0.01 and ****P*<0.001 indicate significant contributions as assessed by Student's *t*-test, compared with reference value 0 (i.e. no contribution to ATP release). Numbers of datasets are indicated. Intervention data used to construct matrices are provided in Tables S5 and S6. B.M., bone marrow; $[Ca^{2+}]_e$, extracellular calcium; $[Ca^{2+}]_i$, intracellular calcium; CFTR, cystic fibrosis transmembrane conductance regulator; endo, endothelial cells; epi, epithelial cells; fibro., fibroblast; FSS, fluid shear stress; Glomer., glomerular; kin., kinase; MSC, mesenchymal stem cells; mTs, microtubules; Pul. Art., pulmonary artery; S.M., smooth muscle; Trab. mesh., trabecular meshwork cells; Um., umbilical; VRAC, volume-regulated anion channel.

mechanisms was limited by overlapping and off-target effects of many inhibitors, as well as lack of within-study inhibitor validation and over-reliance on assumed pharmacological targets. We minimized false-positive outcomes by applying random effects meta-analytic models and considering Bonferroni adjustments for multiple comparison analyses (Glass, 1986). There remains a distinct possibility of false-negative outcomes due to limited sample sizes in some subgroups, aggregation bias and heterogeneity (Higgins and Thompson, 2002).

Quantitative characterization

We estimated that mechanically stimulated mammalian cells release 38.6 (95% CI: 18.2–81.8) amol ATP/cell, resulting in a 4.3-fold (95% CI: 3.8–4.8) increase in ATP above basal levels of 8.1 (95% CI: 3.9–16.6) amol ATP/cell. Intracellular ATP content was estimated to be 3 orders of magnitude higher than basal ATP levels in nucleated cells, 5.0 (95% CI: 2.6–9.5) fmol ATP/cell, and 2 orders of magnitude higher in RBCs, 0.14 (95% CI: 0.12, 0.18) fmol ATP/RBC. Study-level estimates of the absolute amount of ATP released ranged over 10 orders of magnitude, with 5 studies reporting more ATP release than can be contained within a cell, suggesting that more caution must be taken when performing ATP calibrations and measurements, and that basal, released and total ATP content should be reported to obtain relative measures. The characteristic time to half-max ATP release was strongly influenced by the recording method, yielding almost 4 times faster estimates by real-time recordings compared with estimates acquired by bulk sampling and offline measurement. This difference can potentially be explained by the diffusion time required to equilibrate the concentration within the volume of the culture medium. In this regard, the volume into which ATP is released is an important (but not routinely controlled for) determinant of the effective ATP concentration available for autocrine and paracrine signaling, including ATP-regulated ATP release (Bodin and Burnstock, 1996; Dillon et al., 2013). We found that less ATP is released in response to cyclic stimulation; however, no studies reported the kinetics of ATP

Journal of Cell Science (2018) 131, jcs223354. doi:10.1242/jcs.223354

Table 1. Total contribution of the main routes of ATP release

Cell type	Studied mechanisms	Joint contributions (%±95% CI)	Proposed interaction
Astrocytes	Px, Cx, VRAC, MAC	118 (67.8, 168.2)	Additive
Cardiomyocytes	Px, VRAC, MAC	176.6 (140.4, 212.8)	Synergy
Chondrocytes	Vesicle, Px, Cx, MAC	99.2 (32.9, 165.5)	Additive
Ciliary epithelia	Vesicle, Px, Cx, VRAC, MAC	122.1 (39.8, 204.4)	Additive
Keratinocytes	Vesicle, Px, Cx, VRAC, MAC	92.7 (−18.7, 204.1)	Additive
Ligament cells	Px, Cx	146.6 (139.9, 153.3)	Synergy
Mammary epithelia	Vesicle, Px, Cx, VRAC, MAC	53.9 (−64.3, 172.1)	Additive
Pancreatic epithelia	Vesicle, Px	164.3 (144.8, 183.8)	Synergy
Renal epithelia	Vesicle, Px, Cx	220.2 (132.4, 308)	Synergy
Trabecular meshwork	Vesicle, Px, Cx, VRAC, MAC	110.9 (35.3, 186.5)	Additive
Urothelial cells	Vesicle, Px, Cx, VRAC	248.1 (137.6, 358.6)	Synergy

The relative contributions (determined from genetic and pharmacological interventions, see Table S6) of each ATP release route were added together. Contributions that added to 100% (contained by 95% CI) were interpreted as additive, and those exceeding 100% were interpreted as synergistic. Shown are cell types in which at least 4 of the 5 main routes of ATP release were studied, except for cell types that exhibited synergy-like interactions, in which case no restriction was placed on the minimum number of routes studied. Cx, connexins; MAC, maxi-anion channel; Px, pannexins; VRAC, volume-regulated anion channel.

release in response to repeated or cyclical stimulations, even though physiological stimuli are often cyclical (Burr et al., 1996; Eyckmans et al., 2011; Fritton et al., 2000). Of interest, studies in which cell injury was assessed and detected or intentionally induced reported a tendency for higher ATP release. However, the amount of injury-related ATP release never reached amounts expected following cell destruction and was not statistically different from osmotic pressure- or FSS-induced ATP release. Thus, quantitative synthesis of basic science studies employing diverse approaches with complex endpoints is feasible and has allowed us to identify methodological variations of consequence.

Dependence on mechanical stimulus

We compared ATP release induced by 9 different types of mechanical stimulation, including stretch-related stimuli, such as substrate strain, osmotic pressure and tissue distention, and FSS and local membrane deformation. Although all types of mechanical stimulation resulted in the release of comparable amounts of ATP, we found significant differences in the kinetics of ATP release, which were much faster in response to FSS- compared with stretch-related stimuli. In addition, we found that VRAC and possibly pannexins were involved in mediating swell- and strain-induced, but not shear-induced, responses. Finally, MSAR from PKD-afflicted renal epithelia was differentially sensitive to FSS and hypotonic swelling. These results strongly suggest that mammalian cells can discriminate between different types of mechanical stimuli. Theoretical models have previously demonstrated that shear stresses induce more cell membrane deformation than stretch-related stimuli (Lynch and Fischbach, 2014; McGarry et al., 2005). Direct comparison of mechanisms involved in hypotonic pressure-

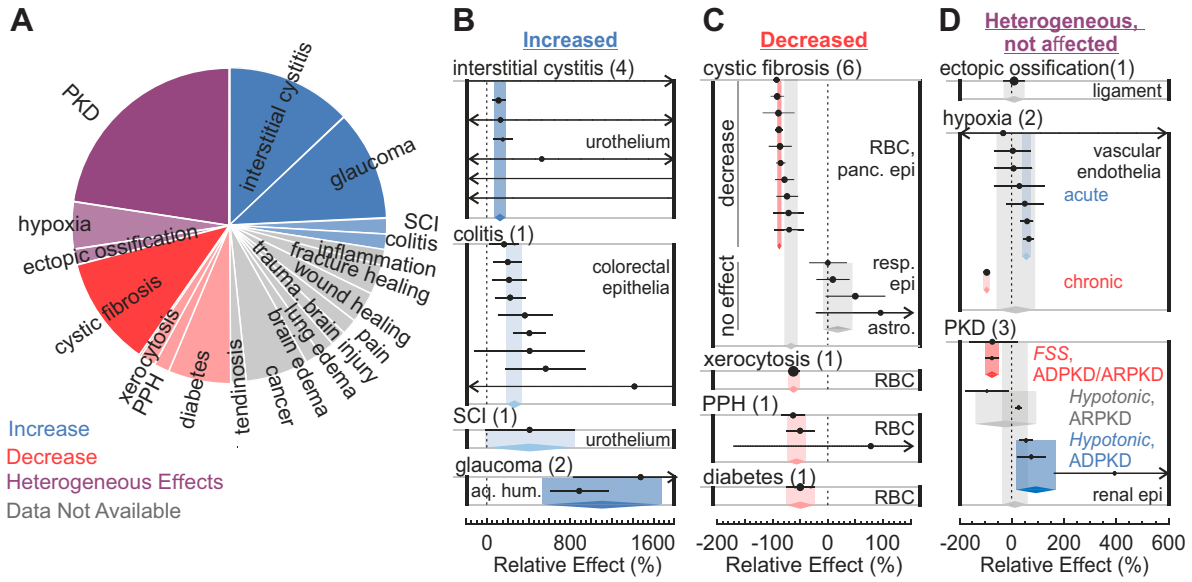

Fig. 6. Pathological ATP release. (A) Pie chart of relative frequency of clinically relevant conditions studied or implicated in aberrant MSAR (61 studies in total). Blue, increased ATP release; red, decreased ATP release; gray, implicated but not measured; purple, heterogeneous effects; light shade, reported by a single study; dark shade, replicated findings. (B–D) Forest plots of relative effect (%) of pathologies (specified at the top left) on MSAR from cells (specified on the right) compared with unaffected controls. Black markers/lines indicate study-level relative effects ±95% CI; bands indicate 95% CI of overall pathology-specific effect. Marker sizes are proportional to study-level sample sizes; numbers of independent studies for each pathology are in parentheses. Black dashed lines are the no effect reference. (B) Pathologies associated with increased MSAR. (C) Pathologies associated with decreased MSAR. (D) Pathologies that had heterogeneous or no effect on MSAR. ADPKD, autosomal dominant PKD; aq. hum., aqueous humour; ARPKD, autosomal recessive PKD; astro., astrocytes; diabetes, type II diabetes; FSS, fluid shear stress; panc. epi, pancreatic epithelia; PKD, polycystic kidney disease; PPH, primary pulmonary hypertension; RBC, red blood cell; resp. epi, respiratory (airway) epithelia; SCI, spinal cord injury.

and strain-induced ATP release has demonstrated that these stretch-related stimuli recruit common ATP release pathways (Li et al., 2011); however, no study has directly compared shear- and stretch-related ATP release. Thus, we recommend a direct comparison between shear- and stretch-induced cell deformation, and ATP release to be investigated in future work.

Intervention studies

We quantified the effects of pharmacological and genetic intervention for 681 combinations of cell type, mechanical stimulation and interventions. From the five main routes of ATP release [vesicular (Bodin and Burnstock, 2001; Sathe et al., 2011), pannexin (Locovei et al., 2006), connexin (Graff et al., 2000), VRAC (Pedersen et al., 1999; Qiu et al., 2014; Voss et al., 2014) and MAC (Sabirov et al., 2001; Sabirov et al., 2017)], at least 2, and often 3, were consistently implicated in the same cell type, with the exception of keratinocytes, in which all 5 pathways were studied, but only MAC was found to mediate ATP release. The involvement of multiple independent release mechanisms may confer a redundancy that ensures that cellular ATP release is robust. Alternatively, it is possible that different routes work collaboratively within the same pathway. Of interest, we demonstrated a lack of additivity in the relative contributions of main release routes in certain cell types. We found that different ATP release routes shared common intracellular signaling pathways. In particular, Rho kinases and microtubules always co-occurred with vesicular and pannexin pathways, and $[Ca^{2+}]_i$ co-occurred with all 5 routes of ATP release in 33–100% of cases. Thus, it can be hypothesized that different routes of release are functionally independent but are regulated by common intracellular signaling. At this time, this hypothesis is difficult to test experimentally, partly because pharmacological agents used to study mechanisms of MSAR suffer from extensively overlapping antagonistic profiles (Azorin et al., 2011; Li et al., 2010; Liu et al., 2008; Sauer et al., 2000; Wang et al., 2005). Targeted genetic studies (e.g. siRNA, CRISPR, animal models) are needed to further our understanding of MSAR. To date, genetic interventions have been used to study the involvement of vesicle-related vesicular nucleotide transporter (VNUT; also known as SLC17A9) (Sathe et al., 2011; Sawada et al., 2008), pannexin 1 (Panx1) (Bao et al., 2004; Beckel et al., 2014; Kanjanamekanant et al., 2014; Lu et al., 2012; Seminario-Vidal et al., 2011; Woehrle et al., 2010), pannexin 2 (Panx2) (Oishi et al., 2012), connexin 40 (Cx40; also known as GJA5) (Toma et al., 2008), connexin 43 (Cx43) (Chi et al., 2014; Genetos et al., 2007; Lu et al., 2012; Luckprom et al., 2011) and connexin 45 (Cx45; also known as GJC1) (Lu et al., 2012). Recently, SWELL1 (also known as LRRC8A) was identified as the pore component of the VRAC complex (Qiu et al., 2014; Syeda et al., 2016; Voss et al., 2014), and the prostaglandin transporter PGT (encoded by *Slco2a1*) was recognized as the MAC (Sabirov et al., 2017). Of interest, Sana-Ur-Rehman et al. (2017) and Workman et al. (2017) have recently reported the calcium homoeostatic modulator 1 (CALHM1) as a novel mediator of MSAR in nasal epithelia and the urothelium; however, it remains unclear whether CALHM1 is a direct or indirect conduit of ATP release. A comprehensive review of recent evidence supporting the role of CALHM1 in ATP release can be found elsewhere (Taruno, 2018). Nonetheless, now that the molecular identity of each main route of ATP release has been identified, genetic studies to resolve ATP release mechanisms are feasible. Thus, systematic analysis of prior data allowed us to pinpoint specific mechanistic features that warrant further experimental investigation, such as differential involvement of VRAC in FSS- and osmotic pressure-induced ATP release, and to suggest that certain ATP release mechanisms are cell type and stimulation type dependent.

Therapeutic potential

Our systematic assessment of MSAR involvement in different pathologies included data from 10 cell types/tissues from 11 pathological conditions. We have found that inflammation and injury coincided with higher ATP release from epithelial cells, which might contribute to pain commonly present in these conditions (Butrick et al., 2010; Docherty et al., 2011; Taweel and Seyam, 2015; Weinreb et al., 2014). In contrast, in hereditary and metabolic conditions, lower ATP release from RBCs was consistently reported. Thus, both MSAR inhibitory and stimulatory interventions can be of therapeutic interest. The downstream actions of MSAR are mediated by 15 members of the purinergic (P2) receptor family (Burnstock, 2014), which have been identified as valuable therapeutic targets for treatment of pain, inflammation, spinal cord injury and bladder dysfunction (North and Jarvis, 2013). There are several advantages of targeting MSAR over the P2 receptor network. First, the impact of disproportionally targeting single P2 receptors has poorly understood implications for signaling by the entire P2 receptor network. Instead, manipulating MSAR allows proportional reduction or increase in the stimulation of all P2 receptors. Second, many of the drugs used to inhibit MSAR, including mefloquine (Lee et al., 2017), carbenoxolone (Doll et al., 1965), probenecid (Li et al., 2016), flufenamic acid (Flemming and Jones, 2015), glybenclamide (Sola et al., 2015) and clodronate (Ghinoi and Brandi, 2002) [recently demonstrated to potently inhibit VNUT (Kato et al., 2017)] are already used in clinic. Although these drugs are relatively non-specific, strategies to therapeutically re-purpose them for diseases with aberrant MSAR may be considered. As for any potential therapy, unintended drug effects need to be taken into account. In this regard, our systematic approach allowed the identification of cell- and stimulus-specific effects of various pathologies. Thus, comprehensive assessment of cell type-specific mechanisms of ATP release, considered together with known pathophysiological changes, can be used to map site-specific effects of therapeutic MSAR interventions, and predict any unintended (patho)physiological consequences.

MATERIALS AND METHODS

Software

Endnote X7 (Thomson Reuters) was used to manage references, the MetaLab meta-analysis toolbox in MATLAB (MathWorks) (N.M. and S.V.K., unpublished) was used for data extraction and analysis, Excel 2016 (Microsoft) was used for data storage and CorelDRAW X8 (Corel) was used for figure preparation.

Search strategy and inclusion criteria

A medical librarian (M.M.) prepared the systematic search strategy. The search strategy was constructed around the key terms ‘ATP’ and ‘mechanical stimulation’. Search terms were validated by ensuring the search retrieved a selection of articles, representative of relevant works. Medline, Embase, Biosis and SCOPUS databases were searched on 12 January 2017, using search terms listed in Table S8, and articles were exported to Endnote. Reviews, books, letters, editorials and conference proceedings were excluded, language was restricted to English and there was no restriction on date of publication. Studies in which mammalian cells were mechanically stimulated and ATP release was assayed were included. No restrictions were imposed on experimental setup. Abstracts were screened independently by two reviewers

(N.M. and A.M.). Full-text screens were conducted to confirm eligibility. Differences between two reviewers were resolved through discussion and consensus. The complete list of systematically identified studies is in Table S9.

Data extraction

Study characteristics and data were extracted by a single non-blinded reviewer (N.M.) and independently verified by another reviewer (A.M.) to minimize user-related error. For all studies, study design and biological characteristics were recorded (Table S10). For experiments using a perfusion-based sampling method, perfusion intervals and volumes were extracted to estimate cumulative ATP release. For experiments reporting outcomes in units other than moles ATP per cell, relevant conversion parameters were extracted. For intervention/pathology studies, we collected information on pharmacological agents, genetic targets or pathological states. MetaLab data extraction module was used to facilitate graphical data extraction (N.M. and S.V.K., unpublished). For each dataset, we extracted baseline ATP levels and mechanically stimulated ATP along with measures of variance. In some studies, multiple datasets were extracted if reported. For temporal recordings of ATP release, entire time series were extracted and used to estimate the time to half-max ATP release for analysis of ATP release kinetics. From these time series, the maximal amount of ATP release was also used for analysis of amount of ATP released. For intervention or pathology studies, basal ATP and amount of ATP released in the absence and presence of the intervention/pathology was extracted for subsequent calculation of the intervention inhibitory effect (%) or relative effect (%) of pathology. Sample sizes and type of variance measures (standard error, standard deviation) used were recorded. When variance measure was unclear, error was extracted as standard error, lending to more conservative estimates. When sample size was unclear but there was indication of multiple trials, we set the sample size to 3. When a range of sample sizes was reported, the smallest value was extracted.

Standardization of measures

ATP was commonly reported as an amount or concentration of ATP released per cell(s). Accordingly, conversion factors were estimated for each study to express ATP amount in terms of moles per cell. In cases in which certain conversion parameters were not reported, assumptions were made according to the table reported in Table S11. Cell-related parameters were estimated using the BioNumbers database (Milo et al., 2010), and were compared with our in-laboratory experience and deemed appropriate. Volume assumptions for culture dishes were made per manufacturer-recommended volumes. For each type of mechanical stimulation, if enough information was provided, magnitude of stimulus was converted to a common unit. Experiments that applied osmotic pressure commonly reported changes in osmolarity as a percentage of basal osmolarity (isotonic). Because basal osmolarity varied across studies, we expressed the magnitude of osmotic stress in terms of change in mOsm/KgH_2O (δ mOsm/l).

Quality assessment

Quality of studies was assessed according to an 8-item quality checklist: publication in peer-reviewed journal, control of temperature, control of sample degradation, cell viability checked, mechanical stimulus regime reported, ATP calibration, negative control and statement of potential conflicts of interest reported. Outcomes were stratified by aggregate quality score to determine the influence of study quality on reported results.

Study-level outcomes

Five outcomes were synthesized in this study: (1) absolute ATP released (A_{mech}), (2) relative ATP released above baseline (R_{mech}), (3) time to half-max ATP release (t_{half}), (4) effect of pharmacological/genetic intervention on ATP release (% inhibition) and (5) effect of pathology on ATP release (relative effect, %).

Study-level absolute ATP release

The amount of ATP released was calculated as the difference in extracellular ATP before and after mechanical stimulation:

$$A_{mech} = A_{EC} - A_{base}, \quad (1)$$

where A_{mech} was mechanically induced ATP release, A_{EC} was total extracellular ATP following mechanical stimulation and A_{base} was basal extracellular ATP.

Study-level relative ATP release

The relative amount of ATP released above baseline R_{mech} was computed as:

$$R_{mech} = \frac{A_{mech} + A_{base}}{A_{base}} \times 100\%. \quad (2)$$

Estimation of cumulative ATP release

Extracted ATP release time series were reported as cumulative ATP release or rates of ATP release. Release rates data were converted to cumulative ATP release over the reported period following mechanical stimulation:

$$A(t) = \int_0^b a(t)dt \approx \sum_1^b (a(t)), \quad (3)$$

where a was the cellular release rate (units ATP per unit time per cell), $A(t)$ was the cumulative extracellular ATP, b was the reported time period and t was the time.

Study-level ATP release kinetics

Study-level ATP release time series recordings with at least 4 time points were fit to a sigmoidal function (Eqn 4) using a Monte Carlo error propagation method, and the characteristic time to half-max release t_{half} with standard error was estimated. Recordings that extended beyond the time of maximal ATP release were truncated to restrict the fitting of the sigmoid curve to the relevant period over which ATP was released.

$$A(t) = \frac{A_{max} \times t^n}{t_{half}^n + t^n}, \quad (4)$$

where A_{max} was maximal ATP release, $A(t)$ was cumulative ATP release with respect to time, n was coefficient related to the slope of activation, t was time and t_{half} was time to half-max release. The Monte Carlo fitting method allowed us to propagate study-level variances (uncertainty in the model inputs) to the uncertainty in the model parameter estimates (Cox et al., 2003). This approach assumes that study-level estimates are normally distributed, enabling pseudo random observations to be sampled from a distribution defined by the study-level means and standard deviations. The pseudo random observations were then averaged to obtain a Monte Carlo estimate for each time point and the sigmoidal model was fit to the Monte Carlo estimates using the least-squared method. This procedure of pseudo-

random sampling and model fitting was iterated 1000 times, and the distribution of 1000 t_{half} estimates was used to compute a mean and variance that was then used as the study-level estimate of t_{half}. Model goodness of fit was assessed quantitatively by R^2 and visually verified.

Study-level percentage inhibition

For intervention studies, the effect of genetic and pharmacological interventions was computed as percentage inhibition, compared with unaffected control of ATP release:

$$\text{inhibition}(\%) = \frac{A_{mech}^{control} - A_{mech}^{treated}}{A_{mech}^{control}} \times 100\%. \quad (5)$$

$A_{mech}^{control}$ and $A_{mech}^{treated}$ were computed the same as A_{mech} (i.e. basal ATP release was accounted for). Negative values of percentage inhibition outcomes indicate increased ATP release, and positive values indicate decreased ATP release.

Study-level relative effects

For pathophysiological conditions, the relative effect size was calculated as follows:

$$\text{effect}(\%) = \frac{A_{mech}^{affected} - A_{mech}^{control}}{A_{mech}^{control}} \times 100\%, \quad (6)$$

where $A_{mech}^{affected}$ was ATP released from the pathologically affected cell/tissue type and $A_{mech}^{control}$ was ATP released from healthy control samples.

Quantitative synthesis

For each study i, study-level outcomes θ_i and standard errors $se(\theta_i)$ were estimated. θ_i is a general study-level outcome used to represent A_{mech}, R_{mech}, t_{half}, inhibition (%) or effect (%).

Data transformation and normalization

Prior to synthesis, skewed distributions of study-level outcomes θ_i were identified by histograms and were normalized by transformation to the logarithmic scale:

$$\Theta_i = log_{10}(\theta_i) - \left(\frac{se(\Theta_i)^2}{2}\right), \quad (7)$$

where Θ_i is a log-transformed (base 10) study-level outcome that we reported in the study as either A_{mech}^{log}, R_{mech}^{log} or t_{half}^{log}. The corresponding standard error $se(\Theta_i)$ was approximated as:

$$se(\Theta_i) = \sqrt{log_{10}\left(\frac{se(\theta_i)^2}{\theta_i^2} + 1\right)}, \quad (8)$$

Log transformation was applied as shown for A_{mech}, R_{mech} and t_{half} datasets. Outcomes were synthesized on the logarithmic scale, transformed back to the original raw scale and reported.

Analysis of heterogeneity

To quantify the extent of inconsistency, or heterogeneity, present between datasets, we calculated Q, I^2 and H^2 heterogeneity statistics. Q is a measure of total variation and was calculated as the sum of the weighted squared differences between the study-level means θ_i and the fixed effect estimate $\hat{\theta}_{FE}$:

$$Q = \sum_{i=1}^{N} (se(\theta_i)^{-2} \times (\theta_i - \hat{\theta}_{FE})^2), \quad (9)$$

where

$$\hat{\theta}_{FE} = \frac{\sum_i se(\theta_i)^{-2}\theta_i}{\sum_i se(\theta_i)^{-2}},$$

Q is a χ^2 distributed statistic with $N-1$ degrees of freedom and the corresponding P-value P_Q was used to evaluate the null hypothesis that all datasets reported the same effect. For example, $P_Q>0.05$ indicates that outcomes are consistent and describe the same effect, whereas $P_Q<0.05$ indicates that outcomes are inconsistent or heterogeneous. H^2 is another heterogeneity metric that is independent of the number of datasets available, and describes the relative excess of Q over the degrees of freedom (d.f.):

$$H^2 = \frac{Q}{\text{d.f.}} \quad (10)$$

I^2 is a transformation of H^2 that describes the percentage of variance that is due to heterogeneity:

$$I^2 = \frac{H^2 - 1}{H^2} \times 100\%. \quad (11)$$

H^2 is preferred over I^2 for highly heterogeneous data because it has an unbound upper limit; however, I^2 is more easily interpretable. Values of Q=0, I^2=0 or H^2=1 indicate that data are homogeneous.

Heterogeneity and publication bias were assessed using funnel plots and cumulative-study exclusion plots. The homogeneity threshold T_H was calculated from cumulative exclusion analysis and specifies the percentage of studies that need to be removed (according to maximal Q-reduction criteria) before a homogenous set of studies is attained, as determined by the P-value P_Q corresponding to the Q heterogeneity statistic (N.M. and S.V.K., unpublished).

Meta-analysis

Study-level outcomes were synthesized under the assumptions of a random effects model to obtain an overall outcome $\hat{\theta}$:

$$\hat{\theta} = \frac{\sum_i (\theta_i \times w_i)}{\sum_i (w_i)}, \quad (12)$$

where the random effects study-level weights w_i were estimated as

$$w_i = \frac{1}{se(\theta_i)^2 + \tau^2} \quad (13)$$

and the interstudy variance was approximated using the DerSimonian–Laird estimator:

$$\tau^2 = \frac{Q - (N-1)}{c}, \quad (14)$$

where

$$c = \sum_i se(\theta_i)^{-2} - \frac{\sum_i (se(\theta_i)^{-2})^2}{\sum_i se(\theta_i)^{-2}}.$$

Q is the heterogeneity statistic (introduced above), c is a scaling factor and N is the number of datasets being synthesized. The standard error corresponding to the overall outcome was estimated as:

$$se(\hat{\theta}) = \frac{1}{\sqrt{\sum_i w_i}} \quad (15)$$

and the corresponding confidence intervals were constructed using critical values $z_{1-\alpha/2}$ obtained from a z-distribution:

$$\pm CI = \pm z_{1-\alpha/2} \times se(\hat{\theta}), \quad (16)$$

where α=0.05 corresponds to a 95% significance level.

Subgroup analyses were conducted to identify sources of heterogeneity and explore the influence of different experimental and biological factors on the outcome of interest. Study-level data were stratified into characteristic groups defined by study-level covariates and study-level outcomes within each subgroup were synthesized as above. When multiple subgroups comparisons were made, the Bonferroni correction was used to adjust the significance threshold to control for false-positive findings:

$$\alpha^* = \frac{\alpha}{m}, \quad (17)$$

where α* is the adjusted significance threshold to attain intended error rates α for m subgroup comparisons.

Meta-regression

To assess the bivariate relationship between study-level predictors and outcomes, a random-effects meta-regression model was constructed in the following form:

$$\theta_i = \beta_0 + \beta_{inter} x_i + \eta_i + \varepsilon_i, \quad (18)$$

where β_0 is the intercept, β_{inter} is the slope coefficient describing the relationship between predictor x_i and outcome θ_i, ε_i is the intrastudy variability approximated by $\mathcal{N}(0,\ se(\theta_i)^2)$ and η_i is the interstudy variability approximated by $\mathcal{N}(0, \tau^2)$. In addition to the meta-regression analysis conducted to assess the between-study relationship of study-level predictors and outcomes, we also conducted an intrastudy regression analysis to assess the within-study relationship between study-level predictors and outcomes (N.M. and S.V.K., unpublished). Within-study regression coefficients were computed and pooled using the meta-analytic methods described above to estimate an overall effect β_{intra}. The magnitude and sign of β_{inter} and β_{intra} were then compared to evaluate whether the observed relationships between and within studies were in agreement.

Analysis of ATP release mechanisms

To evaluate the cell type-specific mechanisms of ATP release, pharmacological and genetic intervention outcomes were grouped by common molecular targets and their inhibitory effects were estimated and synthesized as above. Owing to the non-specific effects of certain inhibitors, differential pharmacological effects were considered to differentiate between ATP release pathways that shared common pharmacological profiles. Depending on the panel of available inhibitor data for each cell type, more targeted interventions allowed us to narrow down the pathways affected by non-specific inhibitors. For example, carbenoxolone inhibits connexin and pannexin activity, while flufenamic acid is a more targeted connexin inhibitor. For cells in which carbenoxolone inhibited ATP release, but flufenamic acid did not, we inferred the involvement of pannexins. In some cases, non-specific interventions were used to support or dismiss the involvement of several pathways at a time. For instance, cells in which Gd^{3+} had no effect on ATP release allowed us to putatively dismiss ATP release pathways related to MACs, P2X7, Piezo1 and transient receptor potential (TRP) channels. To reflect the varying degrees of evidence (i.e. availability of data, specificity of interventions, separate replication of findings), we distinguished between cell type-specific mechanisms that were reported once, those that were verified by different methods/groups, and those for which data were available but inconclusive (often due to the non-specific nature of interventions). These outcomes were summarized in a cell-by-mechanism involvement matrix, indicating whether the pathway was involved in ATP release and the degree of evidence supporting the conclusion. Based on the mechanisms summarized in the involvement matrix, a co-occurrence analysis was then conducted to screen for possibly co-dependent pathways of ATP release. Results were summarized in a co-occurrence matrix for cases in which at least 3 cell types could be evaluated, and were expressed as the percentage of cell types in which the pairs of mechanisms were co-occurrent.

To determine whether the separate routes of ATP release were additive, the effects of ATP release inhibitors were used to approximate of relative contribution (RC) of that pathway to ATP release:

$$RC \sim inhibitory\ effect(\%). \quad (19)$$

The joint contribution (JC) was then computed as:

$$JC = RC_{vesicles} + RC_{px} + RC_{cx} + RC_{VRAC} + RC_{MAC} \quad (20)$$

and the standard error was

$$se(JC) = \sqrt{\begin{array}{c} se(RC_{vesicles})^2 + se(RC_{px})^2 + se(RC_{cx})^2 \\ +se(RC_{VRAC})^2 + se(RC_{MAC})^2 \end{array}} \quad (21)$$

95% CI for joint contributions were constructed using Eqn 16. Joint contributions that were insignificantly different from 100% (contained by 95% CI) were interpreted as additive, and those exceeding 100% were interpreted as synergistic. Cell types in which at least 4 of the 5 main routes of ATP release were studied were included in this analysis, except for cell types that exhibited synergy-like interactions, in which case no restriction was placed on the minimum number of routes studied, because including the relative contributions of additional release routes would have only added to the joint contribution.

Competing interests

The research was conducted in the absence of any commercial or financial relationships that could be construed as a potential conflict of interest.

Author contributions

Conceptualization: N.M., S.V.K.; Methodology: N.M., M.M., S.V.K.; Validation: N.M., A.M., M.M.; Formal analysis: N.M., A.M., S.V.K.; Investigation: N.M.; Resources: M.M.; Data curation: N.M., A.M., S.V.K.; Writing - original draft: N.M., S.V.K.; Writing - review & editing: N.M., A.M., M.M., S.V.K.; Visualization: N.M., S.V.K.; Supervision: S.V.K.; Project administration: S.V.K.; Funding acquisition: S.V.K.

Funding

This work was supported by the Natural Sciences and Engineering Research Council of Canada [RGPIN-288253] and the Canadian Institutes of Health Research [MOP-77643]. N.M. was supported by the Faculty of Dentistry, McGill University and Réseau de Recherche en Santé Buccodentaire et Osseuse.

Supplementary information

Supplementary information available online at
http://jcs.biologists.org/lookup/doi/10.1242/jcs.223354.supplemental

References

Azorin, N., Raoux, M., Rodat-Despoix, L., Merrot, T., Delmas, P. and Crest, M. (2011). ATP signalling is crucial for the response of human keratinocytes to mechanical stimulation by hypo-osmotic shock. *Exp. Dermatol.* **20**, 401-407.

Bao, L., Locovei, S. and Dahl, G. (2004). Pannexin membrane channels are mechanosensitive conduits for ATP. *FEBS Lett.* **572**, 65-68.

Beckel, J. M., Argall, A. J., Lim, J. C., Xia, J., Lu, W., Coffey, E. E., Macarak, E. J., Shahidullah, M., Delamere, N. A., Zode, G. S. et al. (2014). Mechanosensitive

release of adenosine 5′-triphosphate through pannexin channels and mechanosensitive upregulation of pannexin channels in optic nerve head astrocytes: a mechanism for purinergic involvement in chronic strain. *Glia* **62**, 1486-1501.
Bergman, J. (1999). ATP: the perfect energy currency for the cell. *Creation Res. Soc. Q.* **36**, 2-9.
Bodin, P. and Burnstock, G. (1996). ATP-stimulated release of ATP by human endothelial cells. *J. Cardiovasc. Pharmacol.* **27**, 872-875.
Bodin, P. and Burnstock, G. (2001). Evidence that release of adenosine triphosphate from endothelial cells during increased shear stress is vesicular. *J. Cardiovasc. Pharmacol.* **38**, 900-908.
Bradbury, A. and Plückthun, A. (2015). Standardize antibodies used in research: to save millions of dollars and dramatically improve reproducibility, protein-binding reagents must be defined by their sequences and produced as recombinant proteins, say Andrew Bradbury, Andreas Pluckthun and 110 co-signatories. *Nature* **518**, 27-29.
Burnstock, G. (2014). Purinergic signalling: from discovery to current developments. *Exp. Physiol.* **99**, 16-34.
Burr, D. B., Milgrom, C., Fyhrie, D., Forwood, M., Nyska, M., Finestone, A., Hoshaw, S., Saiag, E. and Simkin, A. (1996). In vivo measurement of human tibial strains during vigorous activity. *Bone* **18**, 405-410.
Butrick, C. W., Howard, F. M. and Sand, P. K. (2010). Diagnosis and treatment of interstitial cystitis/painful bladder syndrome: a review. *J. Womens Health (Larchmt)* **19**, 1185-1193.
Chi, Y., Gao, K., Zhang, H., Takeda, M. and Yao, J. (2014). Suppression of cell membrane permeability by suramin: involvement of its inhibitory actions on connexin 43 hemichannels. *Br. J. Pharmacol.* **171**, 3448-3462.
Cox, M., Harris, P. and Siebert, B. R.-L. (2003). Evaluation of measurement uncertainty based on the propagation of distributions using Monte Carlo simulation. *Meas. Tech.* **46**, 824-833.
Dillon, J. P., Vindigni, G., Collins, J., Wilson, P. J., Ranganath, L. R., Milner, P. I. and Gallagher, J. A. (2013). ATP-Stimulated ATP release and metabolic acid production: -regulating life and death decisions in articular chondrocytes. *Osteoarthritis Cartilage* **21**, S111.
Docherty, M. J., Jones, R. C. W. and Wallace, M. S. (2011). Managing pain in inflammatory bowel disease. *Gastroenterol. Hepatol.* **7**, 592-601.
Doll, R., Hill, I. D. and Hutton, C. F. (1965). Treatment of gastric ulcer with carbenoxolone sodium and oestrogens. *Gut* **6**, 19.
Eyckmans, J., Boudou, T., Yu, X. and Chen, C. S. (2011). A hitchhiker's guide to mechanobiology. *Dev. Cell* **21**, 35-47.
Flemming, K. D. and Jones, L. K. (2015). *Mayo Clinic Neurology Board Review: Clinical Neurology for Initial Certification and MOC*: Oxford University Press.
Fontoura-Andrade, J. L., de Amorim, R. F. B. and de Sousa, J. B. (2017). Improving reproducibility and external validity. The role of standardization and data reporting of laboratory rat husbandry and housing. *Acta Cirurgica Brasileira* **32**, 251-262.
Fritton, S. P., McLeod, K. J. and Rubin, C. T. (2000). Quantifying the strain history of bone: spatial uniformity and self-similarity of low-magnitude strains. *J. Biomech.* **33**, 317-325.
Genetos, D. C., Kephart, C. J., Zhang, Y., Yellowley, C. E. and Donahue, H. J. (2007). Oscillating fluid flow activation of gap junction hemichannels induces ATP release from MLO-Y4 osteocytes. *J. Cell. Physiol.* **212**, 207-214.
Ghinoi, V. and Brandi, M. L. (2002). Clodronate: mechanisms of action on bone remodelling and clinical use in osteometabolic disorders. *Expert Opin Pharmacother.* **3**, 1643-1656.
Glass, G. V. (1986). Statistical methods for meta-analysis. Larry V. Hedges, Ingram Olkin. *AJS* **92**, 255-256.
Graff, R. D., Lazarowski, E. R., Banes, A. J. and Lee, G. M. (2000). ATP release by mechanically loaded porcine chondrons in pellet culture. *Arthritis. Rheum.* **43**, 1571-1579.
Higgins, J. P. T. and Thompson, S. G. (2002). Quantifying heterogeneity in a meta-analysis. *Stat. Med.* **21**, 1539-1558.
Jackson, D. and Turner, R. (2017). Power analysis for random-effects meta-analysis. *Res Synth Methods* **8**, 290-302.
Kanjanamekanant, K., Luckprom, P. and Pavasant, P. (2014). P2X7 receptor-Pannexin1 interaction mediates stress-induced interleukin-1 beta expression in human periodontal ligament cells. *J. Periodontal Res.* **49**, 595-602.
Kato, Y., Hiasa, M., Ichikawa, R., Hasuzawa, N., Kadowaki, A., Iwatsuki, K., Shima, K., Endo, Y., Kitahara, Y., Inoue, T. et al. (2017). Identification of a vesicular ATP release inhibitor for the treatment of neuropathic and inflammatory pain. *Proc. Natl Acad. Sci. USA* **114**, E6297-E6305.
Lee, S. J., ter Kuile, F. O., Price, R. N., Luxemburger, C. and Nosten, F. (2017). Adverse effects of mefloquine for the treatment of uncomplicated malaria in Thailand: a pooled analysis of 19, 850 individual patients. *PLoS ONE* **12**, e0168780.
Li, A., Leung, C. T., Peterson-Yantorno, K., Mitchell, C. H. and Civan, M. M. (2010). Pathways for ATP release by bovine ciliary epithelial cells, the initial step in purinergic regulation of aqueous humor inflow. *Am. J. Physiol. Cell Physiol.* **299**, C1308-C1317.
Li, A., Leung, C. T., Peterson-Yantorno, K., Stamer, W. D. and Civan, M. M. (2011). Cytoskeletal dependence of adenosine triphosphate release by human trabecular meshwork cells. *Invest. Ophthalmol. Vis. Sci.* **52**, 7996-8005.
Li, S., Yang, H., Guo, Y., Wei, F., Yang, X., Li, D., Li, M., Xu, W., Li, W., Sun, L. et al. (2016). Comparative efficacy and safety of urate-lowering therapy for the treatment of hyperuricemia: a systematic review and network meta-analysis. *Sci. Rep.* **6**, 33082.
Liu, H.-T., Toychiev, A. H., Takahashi, N., Sabirov, R. Z. and Okada, Y. (2008). Maxi-anion channel as a candidate pathway for osmosensitive ATP release from mouse astrocytes in primary culture. *Cell Res.* **18**, 558-565.
Locovei, S., Bao, L. and Dahl, G. (2006). Pannexin 1 in erythrocytes: function without a gap. *Proc. Natl. Acad. Sci. USA* **103**, 7655-7659.
Lu, D., Soleymani, S., Madakshire, R. and Insel, P. A. (2012). ATP released from cardiac fibroblasts via connexin hemichannels activates profibrotic P2Y2 receptors. *FASEB J.* **26**, 2580-2591.
Luckprom, P., Kanjanamekanant, K. and Pavasant, P. (2011). Role of connexin43 hemichannels in mechanical stress-induced ATP release in human periodontal ligament cells. *J. Periodontal Res.* **46**, 607-615.
Lynch, M. E. and Fischbach, C. (2014). Biomechanical forces in the skeleton and their relevance to bone metastasis: biology and engineering considerations. *Adv. Drug Delivery. Rev.* **79-80**, 119-134.
McGarry, J. G., Klein-Nulend, J., Mullender, M. G. and Prendergast, P. J. (2005). A comparison of strain and fluid shear stress in stimulating bone cell responses–a computational and experimental study. *FASEB J.* **19**, 482-484.
Milner, P., Kirkpatrick, K. A., Ralevic, V., Toothill, V., Pearson, J. and Burnstock, G. (1990). Endothelial cells cultured from human umbilical vein release ATP, substance P and acetylcholine in response to increased flow. *Proc. R. Soc. Lond. Ser. B Biol. Sci.* **241**, 245-248.
Milo, R., Jorgensen, P., Moran, U., Weber, G. and Springer, M. (2010). BioNumbers—the database of key numbers in molecular and cell biology. *Nucleic Acids Res.* **38**, D750-D753.
North, R. A. and Jarvis, M. F. (2013). P2X receptors as drug targets. *Mol. Pharmacol.* **83**, 759-769.
Oishi, S., Sasano, T., Tateishi, Y., Tamura, N., Isobe, M. and Furukawa, T. (2012). Stretch of atrial myocytes stimulates recruitment of macrophages via ATP released through gap-junction channels. *J. Pharmacol. Sci.* **120**, 296-304.
Pedersen, S., Pedersen, S. F., Nilius, B., Lambert, I. H. and Hoffmann, E. K. (1999). Mechanical stress induces release of ATP from Ehrlich ascites tumor cells. *Biochim. Biophys. Acta* **1416**, 271-284.
Qiu, Z., Dubin, A. E., Mathur, J., Tu, B., Reddy, K., Miraglia, L. J., Reinhardt, J., Orth, A. P. and Patapoutian, A. (2014). SWELL1, a plasma membrane protein, is an essential component of volume-regulated anion channel. *Cell* **157**, 447-458.
Sabirov, R. Z., Dutta, A. K. and Okada, Y. (2001). Volume-dependent Atp-conductive large-conductance anion channel as a pathway for swelling-induced Atp release. *J. Gen. Physiol.* **118**, 251-266.
Sabirov, R. Z., Merzlyak, P. G., Okada, T., Islam, M. R., Uramoto, H., Mori, T., Makino, Y., Matsuura, H., Xie, Y. and Okada, Y. (2017). The organic anion transporter SLCO2A1 constitutes the core component of the Maxi-Cl channel. *EMBO J.* **36**, 3309-3324.
Sana-Ur-Rehman, H., Markus, I., Moore, K. H., Mansfield, K. J. and Liu, L. (2017). Expression and localization of pannexin-1 and CALHM1 in porcine bladder and their involvement in modulating ATP release. *Am. J. Physiol. Regul. Integr. Comp. Physiol.* **312**, R763-R772.
Sathe, M. N., Woo, K., Kresge, C., Bugde, A., Luby-Phelps, K., Lewis, M. A. and Feranchak, A. P. (2011). Regulation of purinergic signaling in biliary epithelial cells by exocytosis of SLC17A9-dependent ATP-enriched vesicles. *J. Biol. Chem.* **286**, 25363-25376.
Sauer, H., Hescheler, J. and Wartenberg, M. (2000). Mechanical strain-induced Ca(2+) waves are propagated via ATP release and purinergic receptor activation. *Am. J. Physiol. Cell Physiol.* **279**, C295-C307.
Sawada, K., Echigo, N., Juge, N., Miyaji, T., Otsuka, M., Omote, H., Yamamoto, A. and Moriyama, Y. (2008). Identification of a vesicular nucleotide transporter. *Proc. Natl. Acad. Sci. USA* **105**, 5683-5686.
Seminario-Vidal, L., Okada, S. F., Sesma, J. I., Kreda, S. M., van Heusden, C. A., Zhu, Y., Jones, L. C., O'Neal, W. K., Penuela, S., Laird, D. W. et al. (2011). Rho signaling regulates pannexin 1-mediated ATP release from airway epithelia. *J. Biol. Chem.* **286**, 26277-26286.
Soehnlein, O. and Silvestre-Roig, C. (2017). Basic research: standardizing animal atherosclerosis studies to improve reproducibility. *Nat. Rev. Cardiol.* **14**, 574.
Sola, D., Rossi, L., Schianca, G. P. C., Maffioli, P., Bigliocca, M., Mella, R., Corlianò, F., Fra, G. P., Bartoli, E. and Derosa, G. (2015). Sulfonylureas and their use in clinical practice. *Arch. Med. Sci.* **11**, 840-848.
Syeda, R., Qiu, Z., Dubin, A. E., Murthy, S. E., Florendo, M. N., Mason, D. E., Mathur, J., Cahalan, S. M., Peters, E. C., Montal, M. et al. (2016). LRRC8 proteins form volume-regulated anion channels that sense ionic strength. *Cell* **164**, 499-511.
Taruno, A. (2018). ATP release channels. *Int. J. Mol. Sci.* **19**, 808.
Taweel, W. A. and Seyam, R. (2015). Neurogenic bladder in spinal cord injury patients. *Res. Rep. Urol.* **7**, 85-99.

Toma, I., Bansal, E., Meer, E. J., Kang, J. J., Vargas, S. L. and Peti-Peterdi, J. (2008). Connexin 40 and ATP-dependent intercellular calcium wave in renal glomerular endothelial cells. *Am. J. Physiol. Regul. Integr. Comp. Physiol.* **294**, R1769-R1776.

Voss, F. K., Ullrich, F., Munch, J., Lazarow, K., Lutter, D., Mah, N., Andrade-Navarro, M. A., von Kries, J. P., Stauber, T. and Jentsch, T. J. (2014). Identification of LRRC8 heteromers as an essential component of the volume-regulated anion channel VRAC. *Science* **344**, 634-638.

Wang, E. C. Y., Lee, J.-M., Ruiz, W. G., Balestreire, E. M., von Bodungen, M., Barrick, S., Cockayne, D. A., Birder, L. A. and Apodaca, G. (2005). ATP and purinergic receptor-dependent membrane traffic in bladder umbrella cells. *J. Clin. Investig.* **115**, 2412-2422.

Weinreb, R. N., Aung, T. and Medeiros, F. A. (2014). The pathophysiology and treatment of glaucoma: a review. *JAMA* **311**, 1901-1911.

Woehrle, T., Yip, L., Manohar, M., Sumi, Y., Yao, Y., Chen, Y. and Junger, W. G. (2010). Hypertonic stress regulates T cell function via pannexin-1 hemichannels and P2X receptors. *J. Leukoc. Biol.* **88**, 1181-1189.

Workman, A. D., Carey, R. M., Chen, B., Saunders, C. J., Marambaud, P., Mitchell, C. H., Tordoff, M. G., Lee, R. J. and Cohen, N. A. (2017). CALHM1-mediated ATP release and ciliary beat frequency modulation in nasal epithelial cells. *Sci. Rep.* **7**, 6687.

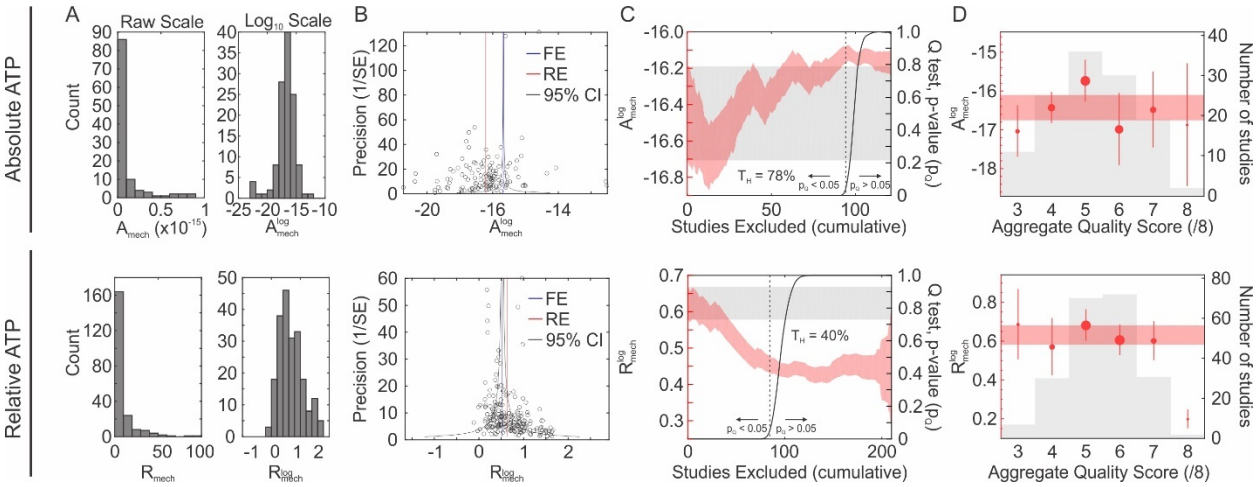

Figure S1. The distribution, bias, extent of heterogeneity and effect of study quality was evaluated for mechanically-stimulated ATP release (A_{mech}, *top row*) and relative ATP release above baseline (R_{mech}, *bottom row*) (A) Study-level outcome distributions on raw scale (*left*) and logarithmic (base 10) scale (*right*). **(B)** Funnel plots for log-transformed study-level effect sizes. *Black markers*: study-level data. *Blue lines*: fixed effect (FE) estimate. *Red lines*: random effects (RE) estimate. *Black lines*: theoretical 95% CI for FE estimate in absence of bias. **(C)** Effect of cumulative study exclusion on RE estimates and heterogeneity of log-transformed effect sizes. *Red band*: 95% CI for studies remaining after exclusion of the most heterogenous. *Grey band*: Overall 95% CI. *Black curve*: p-value p_Q for Q-test. *Dashed black line*: homogeneity threshold T_H. **(D)** Influence of aggregate study quality score on ATP release estimates. *Red band*: 95% CI for overall estimate, *red markers*: score-specific estimate ± 95% CI, *grey bars*: number of studies that received indicated aggregate quality score (also reflected in marker sizes).

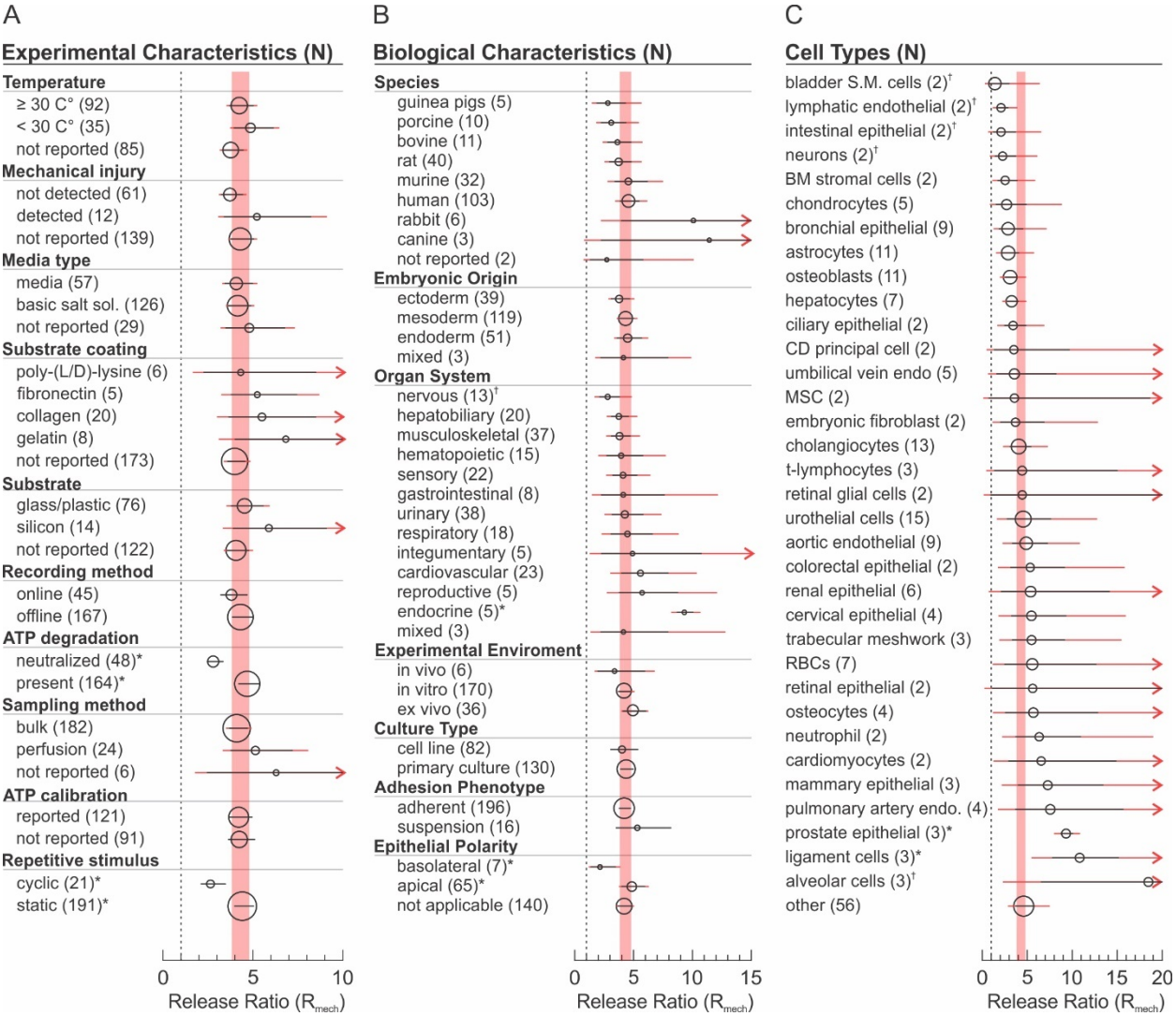

Figure S2. Influence of experimental and biological factors on the amount of ATP released following mechanical stimulation. Shown are estimates of relative ATP release above baseline following mechanical stimulation for different subgroups based on **(A)** experimental characteristics, **(B)** biological characteristics and **(C)** cell-types. *Round markers*: Subgroup-level estimates, markers sizes are proportional to number of datasets N in each subgroup (shown in parentheses), *Horizontal black lines*: ± 95% CI, *Horizontal red lines*: ± Bonferroni-adjusted 95% CI, *Red bands*: overall estimate ± 95% CI. † and * indicate significant differences ($p<0.05$) compared to overall estimate or to other subgroup (in case of two subgroups) before and after Bonferroni adjustment, respectively. Detailed statistics are in **Table S2**.

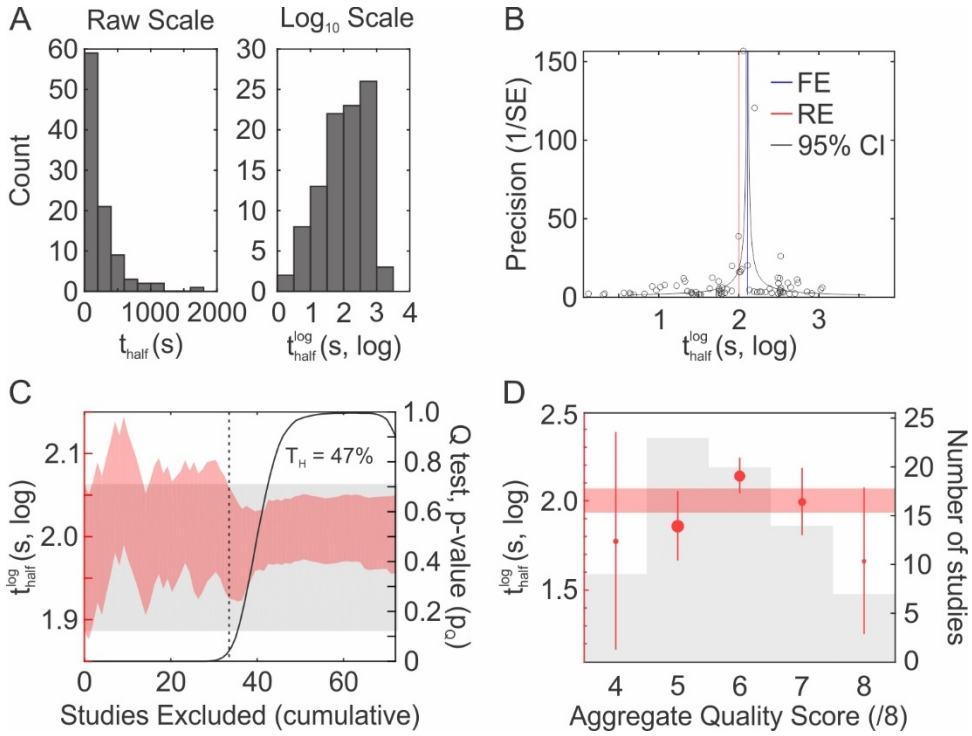

Figure S3. The distribution, bias, extent of heterogeneity and effect of study quality was evaluated for kinetic estimates of ATP release (t_{half}) (A) Study-level effect size distributions on raw scale (*left*) and logarithmic (base 10) scale (*right*). **(B)** Funnel plots for log-transformed study-level estimates. *Black markers*: study-level data. *Blue lines*: fixed effect (FE) estimate. *Red lines*: random effects (RE) estimate. *Black lines*: theoretical 95% CI for FE estimate in absence of bias. **(C)** Effect of cumulative study exclusion on RE estimates and heterogeneity of log-transformed effect sizes. *Red band*: 95% CI for studies remaining after exclusion of most heterogenous. *Grey band*: Overall 95% CI. *Black curve*: p-value p_Q for Q-test. *Dashed black line*: homogeneity threshold T_H. **(D)** Influence of aggregate study quality score on ATP release kinetic estimates. *Red band*: 95% CI for overall estimate, *red markers*: score-specific estimate ± 95% CI, *grey bars*: number of studies that received indicated aggregate quality score (also reflected in marker sizes).

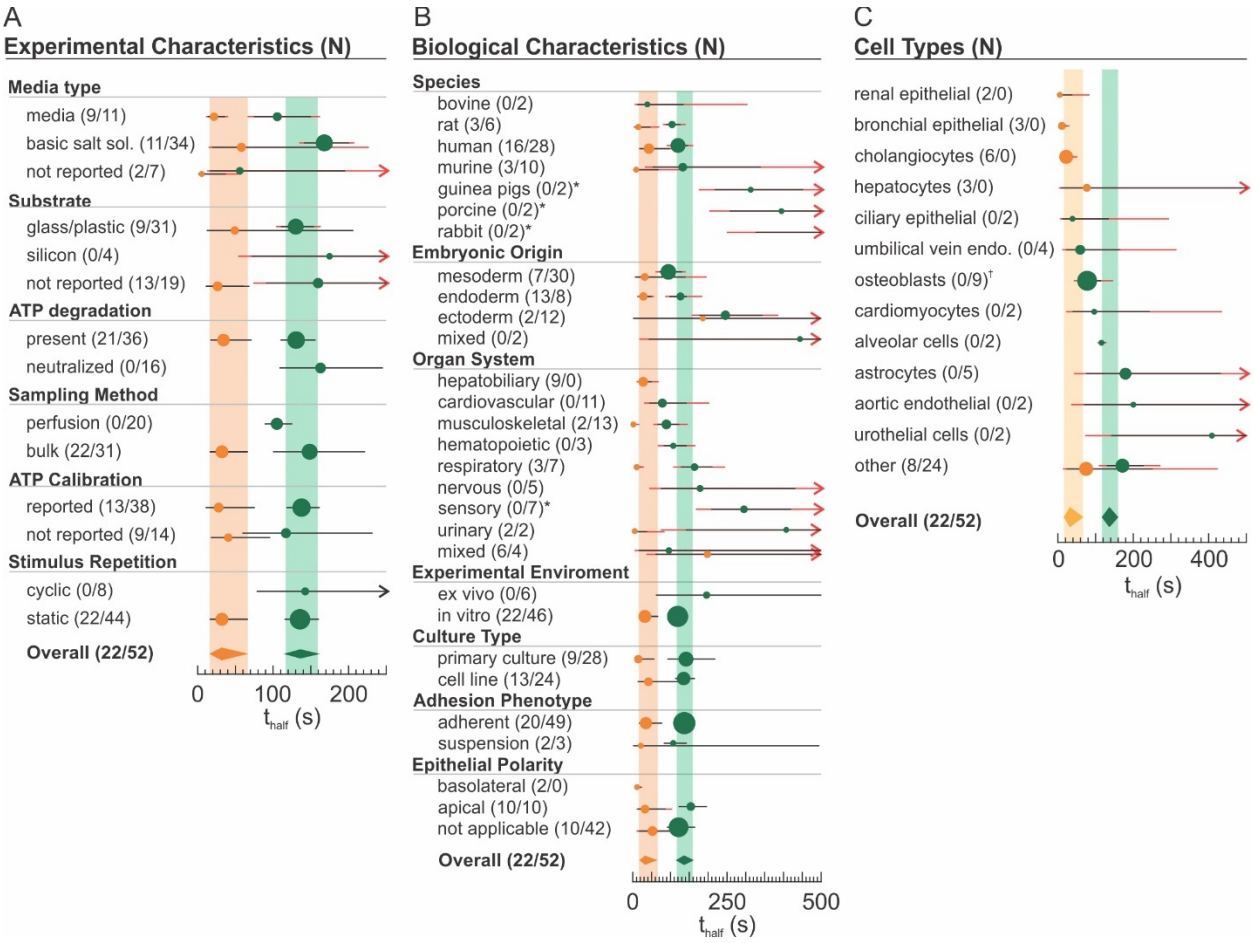

Figure S4. Influence of experimental and biological factors on kinetics of mechanically-stimulated ATP release. (A-E) ATP release kinetic estimates were stratified by online (*orange*) and offline (*green*) recording methods and subgroup analysis was conducted to evaluated influence of experimental **(A)** and biological **(B)** characteristics as well as differences between cell-types **(C)**. *Round markers*: Subgroup-level estimates, *Horizontal black lines*: ± 95% CI, *Horizontal red lines*: ± Bonferroni-adjusted 95% CI, *Bands/diamonds*: overall estimate ± 95% CI. Markers are proportional to number of studies N in each subgroup (shown in parentheses). † and * indicate significant differences (at least 5% level) compared to overall estimate before and after Bonferroni adjustment, respectively. Detailed statistics are in **Table S4**.

Table S1. Absolute estimates of ATP released from mechanically-stimulated mammalian cells (A_{mech}), intracellular ATP (A_{cell}), and basal extracellular ATP (A_{base}). Shown are meta-analytic outcomes and corresponding heterogeneity statistics I^2, H^2 and Q. CI: Confidence intervals, N: Number of datasets, P_Q: p-value corresponding to Q heterogeneity statistic used to evaluate null hypothesis that all studies reported same effect, Nucleated: Nucleated mammalian cells, RBC: Red blood cells.

	Meta-Analysis Summary Statistics					
	ATP released (± 95% CI), units	N	I^2 (%)	H^2	Q	P_Q
A_{mech}	38.5 (18.2, 81.8) amol cell^{-1}	123	99.9	1695.4	206843.1	<0.001
A_{cell}						
Nucleated	5.0 (2.6, 9.5) fmol cell^{-1}	4	89.2	9.2	27.7	<0.001
RBC	0.14 (0.12, 0.18) fmol cell^{-1}	4	0	0.5	1.6	0.66
A_{base}	8.1 (3.9, 16.6) amol cell^{-1}	84	99.8	657.9	54601.8	<0.001

Table S2. Subgroup analysis of the effects of experimental and biological factors on amount of ATP released following mechanical stimulation. Relative ATP release data were stratified by experimental or biological characteristics, or cell type, and amount of ATP released and heterogeneity was compared between subgroups. R_{mech}: relative ATP release compared to baseline, CI: confidence intervals, P_Q: p-value corresponding to Q heterogeneity statistic used to evaluate null hypothesis that all studies reported same effect, N: number of datasets per group.

Click here to Download Table S2

Table S3. Relationship between magnitude of mechanical stimulus and amount of ATP release evaluated by subgroup and meta-regression analyses. *For subgroup analysis*, Relative ATP release data were stratified by type of mechanical stimulus and amount of ATP released and heterogeneity was compared between subgroups. R_{mech}: relative ATP release compared to baseline. P_Q: p-value corresponding to Q heterogeneity statistic used to evaluate null hypothesis that all studies reported same effect. *For meta-regression*, strength of relationship (regression slope, β) was investigated between the magnitude of mechanical stimulus and the amount of relative ATP released on logarithmic scale. Magnitude of stimuli were % stretch for strain, cmH_2O for compression, absolute change in mOsm/L for hypotonic and hypertonic pressures, $dyne/cm^2$ for fluid shear stress (FSS) and μm^{-1} for RBC deformation. Regression slopes were compared between relationships observed within-studies (β_{intra}) and between-studies (β_{inter}). SE(β): standard error of β, P_β: Z-test derived p-value for comparison of β_{inter} and β_{intra}. N: Number of datasets per group.

Click here to Download Table S3

Table S4. Subgroup analysis of the effects of experimental and biological factors on ATP release kinetics. ATP release kinetics data were stratified by experimental or biological characteristics, cell type, or mechanical stimulus, and kinetics of ATP release and heterogeneity were compared between subgroups. t_{half}: Time to half max release, CI: confidence intervals, P_Q: p-value corresponding to Q heterogeneity statistic used to evaluate null hypothesis that all studies reported same effect, N: number of datasets per group.

Click here to Download Table S4

Table S5. Pharmacological Interventions used to study mechanically-stimulated ATP release. *Bolded interventions* are pharmacological agents that do not overlap with other known mechanisms of MSAR. Uncommon or unverified pharmacological interventions have been omitted. Drug pharmacology was obtained from literature identified in the current study.

Target	Pharmacological interventions
Release mechanisms	
Vesicular	**NEM**, **bafilomycin**, **monensin, brefeldin A**
Pannexins	carbenoxolone, 18α/β-glycyrrhetinic acid, probenecid, **10panx1**, NPPB, SITS, **DTT**, mefloquine
Connexins	carbenoxolone, 18 α/β -glycyrrhetinic acid, **octanol**, **heptanol, flufenamic acid** (little activity at Panx1)**,** arachidonic acid, mefloquine, **GAP26**, **GAP27**
VRAC	**tamoxifen**, **fluoxetine**, glybenclamide, **phloretin,** NPPB, SITS, **verapamil**
Maxi-anion	Gd^{3+}, NPPB, SITS, arachidonic acid
Auxiliary mechanisms	
ANK	probenecid
ATP synthase	**angiostatin, piceatannol**
CFTR	glybenclamide, **CFTR-172, Rp-cAMPS, niflumic acid**
ENaC	**amiloride**
L-type VSCC	**nifedipine**
P2X7	**brilliant blue G**, Gd^{3+}, **KN62, A10606120, A438079, A74003**
Piezo1	ruthenium red, Gd^{3+}, **GsMTx4**
TRPV4	**HC067047**, ruthenium red, Gd^{3+}
Regulatory mechanisms	
Intracellular Calcium	**BAPTA-AM, EGTA-AM, thapsigargin**
Extracellular Calcium	Calcium-free (Calcium omitted in solution, optionally chelated)
COX	**etodolac, indomethacin, NS398, ETYA**
PKC	**calphostin C, chelerythrine, myristoylated PKC ζ pseudosubstrate, GF 109203X, Gö6976, Gö6983**
P38 mitogen-activated protein	**SB203590**
Rho kinase	**Y27632, GSK269962, H1152**
MLC kinase	**ML-7**
Tyrosine kinase	**herbimycin A, tyrphostin 46**
PI3K	**wortmannin, LY294002**
f-actin	**cytochalasin B, cytochalasin D**
microtubules	**nocodazole**
cholesterol	**MβCD**
cilia	**chloral hydrate**

Table S6. Mechanisms of mechanically-stimulated ATP release. The effects of pharmacological and genetic interventions on MSAR for studied cell types were calculated as an inhibitory effect (%) ± 95% confidence intervals (CI) compared to vehicle control, according to random effects meta-analysis model. Positive effects (>0%) indicate that MSAR was inhibited and negative effects (<0%) indicate that MSAR was potentiated. Interventions for which 0% was not included in the 95% CI had a significant effect on MSAR. Involvement of studied mechanism in MSAR is indicated by green box (involved) or red box (not involved), and quality of evidence is indicated by dark green/red (finding replicated by separate study/method) or light green/red (not-replicated). Orange boxes: Interventions with inconsistent effects, reasoning for each case is provided in table. P_Q: p-value corresponding to Q heterogeneity statistic used to evaluate null hypothesis that all studies reported same effect, N: number of datasets. *indicates the interventions that were activators or agonists of MSAR, and therefore were not pooled with inhibitory interventions for calculation of overall inhibition.

Click here to Download Table S6

Table S7. ATP release in pathologies. Relative effect (%) of pathology on ATP release compared to unaffected controls. $D_{\downarrow\uparrow}$: specifies direction of effect, CI: 95% confidence intervals, N: number of datasets per condition, I^2 and H^2: heterogeneity statistics, P_Q: p-value corresponding to Q heterogeneity statistic used to evaluate null hypothesis that all studies reported same effect, ADPKD: autosomal dominant polycystic kidney disease, ARPKD: autosomal recessive polycystic kidney disease, CF: cystic fibrosis, Epi.: epithelia, Glaucoma: primary acute angle closure glaucoma, FSS: fluid shear stress, RBC: red blood cells.

Covariates	Meta-Analysis Summary Statistics					
	$D_{\downarrow\uparrow}$	Rel. Effect, % (±95% CI)	N	I^2 (%)	H^2	P_Q
Pathology						
Cystic fibrosis	↓	-66.6 (-78.6, -54.5)	14	87.9		<0.001
RBC, pancreatic epi.	↓	-87.7 (-91.5, -83.8)	10	7.9	1.1	0.37
Airway epi., astrocyte	-	18.1 (-8.5, 44.7)	4	29.1	1.4	0.24
Colitis*	↑	248.1 (172.4, 323.8)	9	19.4	1.2	0.27
Diabetes, type II	↓	-49.6 (-75.0, -24.1)	1	-	-	-
Glaucoma	↑	1107.8 (539.0, 1676.6)	2	62.5	2.7	0.1
Hypoxia	-	20.3 (-55.9, 96.5)	8	97.4	37.8	<0.001
Acute hypoxia*	↑	60.9 (46.4, 75.4)	7	0	0.8	0.53
Chronic hypoxia	↓	-91.8 (-103.4, -80.2)	1	-	-	-
Ectopic ossification	-	4.5 (-38.4, 47.5)	1	-	-	-
Interstitial cystitis	↑	107.7 (53.3, 162.0)	7	0		0.99
Polycystic kidney disease	-	7.8 (-43.1, 58.8)	7	92.5	13.3	<0.001
FSS – AD/ARPKD	↓	-72.9 (-98.9, -46.9)	2	0	<0.001	1
Hypotonic – ADPKD	↑	92.9 (15.0, 170.7)	3	75.5		0.13
Hypotonic – ARPKD	↓	-25.2 (-147.8, 97.3)	2	88.2		<0.01
Pulmonary hypertension *	↓	-56.6 (-73.0, -40.2)	3	0	0.8	0.43
Spinal cord injury	↑	399.2 (-40.3, 838.6)	1	-	-	-
Xerocytosis, hereditary	↓	-61.9 (-71.9, -51.9)	1	-	-	-

*Pooled datasets are from same study

Table S8. Search Strategy

Click here to Download Table S8

Table S9. Systematically identified studies and their contributions to meta-analysis.

Click here to Download Table S9

Table S10. List of study-level characteristics extracted for each study and used in subgroup analyses

Click here to Download Table S10

Table S11: Experimental parameter assumptions for ATP unit conversion. *Top table* describes how unavailable (output) parameters were calculated based on available (input) parameters and assumed parameter values (assumption). Assumed cell-related parameters are shown in *middle table*, and culture dish-dependent parameters shown in the *bottom table*.

Input parameter(s)	Assumed parameter	Calculation	Output parameter
Cytocrit/hematocrit (CC, %), total volume (TV)	Cell volume (CV)	N = (CC x TV) / CV	Cell number (N)
Protein mass (PM)	Protein / cell (PC)	N = PM / PC	Cell number (N)
DNA mass (DM)	DNA / cell (DC)	N = DM / DC	Cell number (N)
Confluence (C, %), surface area (SA)	Confluent Cell Density (D)	N = SA x C x D	Cell number (N)
Culture Plate	Volume (V)	V	Volume (V)

Assumed parameters	Assumed values
Protein / cell (PC)	320 (pg/cell)
Mammalian cell volume (CV)	2.41 (pL)
RBC volume (CV)	0.10 (pL)
Platelet volume (CV)	0.10 (pL)
Cellular density at confluence (D)	10^5 cells / cm^2

Culture Dish	Surface area (SA, cm^2)	Assumed parameters Volume (V, mL)
10 cm	55	10
6 well (35mm)	9.6	2
48 well	1	1
96 well	0.3	0.2